SYNTHESIS AND CHARACTERIZATION OF ACTIVATED CARBON PREPARED FROM PALM SEEDS AND APPLICATIONS FOR 4- CHLOROPHENOL REMOVAL FROM AQUEOUS SOLUTION

BY

Saeed Mohammad Al-Ghamdi

A Thesis Presented to the

DEANSHIP OF GRADUATE STUDIES

KING FAHD UNIVERSITY OF PETROLEUM & MINERALS

DHAHRAN, SAUDI ARABIA

In Partial Fulfillment of the
Requirements for the Degree of

MASTER OF SCIENCE

In

Chemical Engineering

April 2011

King Fahd University of Petroleum & Minerals DHAHRAN
OF GRADUATE STUDIES

DEANSHIP OF GRADUATE STUDIES

The thesis, written by **SAEED MOHAMMAD AL-GHAMDI** under the direction of his thesis advisor and approved by his thesis committee, has been presented to and accepted by the Dean of Graduate Studies, in partial fulfillment of the requirement for the degree of **MASTER OF SCIENCE IN CHEMICAL ENGINEERING.**

Thesis Committee

Dr. R. A. Shawabkeh
Advisor

Dr. M. A. Al-Harthi
Co-Advisor

Dr. Usamah A. Al-Mubaiyedh
Department Chairman

Dr. I. A. Hussein
Member

Dr. Salam A. Zummo
Dean of Graduate Studies

Dr. M. A. Atieh
Member

21/5/11
Date

Dr. M. S. Ba-Shammakh
Member

DEDICATION

This thesis is dedicated to my family who has supported me all the way since starting pursuing my degree as part time. Also, this thesis is dedicated to my academic advisor, thesis advisor and friends who have been great source of motivation and inspiration.

ACKNOWLEDGEMENTS

All thanks and merits are to Allah for his guidance and continue support for me to start and complete this thesis. Also, acknowledgment is for King Fahd University of Petroleum & Mineral for funding and supporting this research.

I would like to express my profound appreciation to my thesis committee chairman Dr. R. A.Shawabkeh for his support, valuable advice, encouragement and his unlimited accessibility. In addition, I would like to thank him for his recommendations to overcome all challenges and obstacles to complete my research.

Moreover, I want to express my appreciation to my committee members; Dr. M. Al-Harthi, Dr. M. Ba-Shammakh, Dr. I. Hussein and Dr. M. Atieh. Gratitude is extended to Dr. Mamdouh Al-Harthi who facilitated conducting my thesis defense. Also, I want to thank him for assisting me in performing my analysis for activated carbon samples.

I wish to thank all workshops and Chemical Engineering department for their help and support. Finally, I want to thank graduate students for their useful suggestions and comments.

TABLE OF CONTENTS

List of Tables

List of Figures

THESIS ABSTRACT

FULL NAME OF STUDENT	**Saeed Mohammad Al-Ghamdi**
TILTED OF STUDY	**Synthesis and Characterization of Activated Carbon Prepared from Palm Seeds and Applications for 4-Chlorophenol Chloride Removal from Aqueous Solution**
MAJOR FIELD	**Chemical Engineering**
DATE OF DEGREE	**April 2011**

Environmental pollution is nowadays one of the most important challenges that are facing humanity. It has been increasing dramatically in the last few years and reached an alarming point. Volatile Organic Compounds (VOC) are considered among the most important pollutants that hazard human and animals' lives. Wastewater containing VOCs such as 4-Chlorophenol, leads to water pollution even in trace amount.

Therefore, in this thesis it was goal to produce activated carbon from palm seeds which high surface area and pore size distribution. Seventy one treatment method for the palm seeds including both physical and chemical activation methods were performed in this research. It was found that the raw material that treated with phosphoric acid using physical activation at 550 ^{o}C for 30 minutes while the flow rate of carbon dioxide 0.8 ml/min shows the best surface area of 1440 m^2/g. The yield of this sample was 93.88 % compared to those treated with phosphoric, sulfuric and nitric acid (73.43%). Scanning Electron Microscope (SEM) showed that this activated carbon contains oxygen and phosphorous functional groups which provides evidence that the carbon surface has been enriched with oxygen and phosphorous functional groups. Also, zero point of charge (ZPC) for this activated carbon was 4.89 at zero pH value. On the other hand, FTIR (Fourier Transform Infrared

Spectroscopy) showed the presence of carboxylic functional groups, aromatic functional groups on the surface of the prepared activated carbon.

This sample was further tested for its adsorption capacity against 4-chlorophenol and showed a maximum adsorption capacity of (17 mg/g). The previous adsorption capacity was achieved with 60 minutes adsorption which represents 8.5 % of the initial concentration. The isotherm model was fitted using BET, Langmuir and Freundlich isotherm and found that BET is the best fit for these data with regression coefficient of 0.98. Also, it was found that 4-CP adsorption on this activated carbon surface is endothermic process.

ملخص الرسالة

الاســــــــم: سعيد محمد الغامدي

عنوان الرسالة: إنتاج الكربون المنشط من نوى التمر ودراسة خصائصة لإستخدامه في إزاله رابع كلوريد الفينول.

التخصـــــص: الهندسة الكيمائية

تاريخ التخـرج: آبريل 2011

التلوث البيئي في الوقت الحاضر هو واحد من أهم التحديات التي تواجه البشرية. وقد تزايد بشكل كبير خلال السنوات القليلة الماضية و وصل إلى نقطة مثيرة للقلق نتيجةً لآثاره الصحية و الاقتصادية على البشرية والبيئة. تعتبر المركبات العضوية المتطايرة من بين أهم الملوثات التي تشكل خطرا على حياة الإنسان و الحيوان. المياه العادمة التي تحتوي على المركبات العضوية المتطايرة مثل رابع كلوريد الفينول تؤدي الى تلوث المياه حتى ولو كانت على مستوى تركيز منخفض.

في هذا البحث كان الهدف هو إنتاج الكربون المحفز من نوى التمر باستخدام كلتا الطريقتين للتحفيز (الكيمائية والفيزيائية) ولقد تم إكتشاف أن الكربون المحفز بوساطة حمض الفسفور عند درجة حرارة 550 رجة مئوية ومعدل 0.8 لتر / دقيقة من غاز ثاني أكسيد الكربون هو الأعلى من حيث مساحة السطح مقارنة بذالك الكربون المفز بواسطة حمض النتريك والفسفور والكبريت أو النتريك والفسفور .

وكان معدل الإنتاج من هذا الكربون هو 93.88 % و لقد أثبت اختبار المسح الإلكتروني وجود الأكسجين والفسفور على سطح هذا الكربون مما يدل على أنه تم تحفيزة بهذين العنصرين خلال عملية التحفيز ولقد كان نقطة الشحنة الصفرية هي 4.89 .على الطرف الآخر ، أثبت المسح المجهري بواسطة الأشعة تحت الحمراء وجود الزمر العطرية على سطح هذا الكربون .

ولقد تم أختيار هذا الكربون المنشط لإزالة رابع كلوريد الفينول من الماء وكانت الطاقة الامتصاصية هي 17 ملجرام لكل جرام من هذا الكربون خلال ساعة . وأخيراً لقد كانت عملية الامتزاز لرابع كلوريد الفينور عملية منتجة للحرارة.

CHAPTER 1

1. INTRODUCTION

Environmental pollution is nowadays one of the most important challenges that are facing humanity. It has been increasing dramatically in the last few years and reached an alarming point in terms of its health and economic impacts on the humanity and environment. Volatile Organic Compounds (VOC) are considered among the most important pollutants that hazard human and animals' lives. Wastewater containing VOCs such as 4-Chlorophenol (4-CP) leads to water pollution even in trace amount. If these toxins could not properly dispose or treated, they may enter the water sources such as ground water, rivers, lakes or reservoirs. Once these contaminates enter the food chain they will affect human health and causing prolonged diseases.

Chlorophenols have strong resistance to physical, chemical or biological treatments, which have a hazardous influence to living organisms including human beings [1]. Exposure to these compounds can occur in workplace, through environmental media, contaminated drinking water and foodstuff or even from the use of consumer products containing phenol. It is well known that most chlorinated compounds, in general, are toxic due to the chlorine contained in their structure. Once they enter into the food chain they cause leukemia in rats and liver cancer in mice, suggesting that 2,4,6-trichlorophenol may be a carcinogen. The acceptable daily intake (ADI) from 4-chlorophenol is 0.1 mg/Kg body weight per day [2].

Removing these pollutants or decreasing their concentration levels in the environment to allowable or permitted levels is a target that needs to be achieved and reached by several environmental agencies and governments. Several treatment methods are available and can be used to treat and remove these pollutants from the environment. They varied according to the type of pollutants. For examples, organics can be removed by chemical and thermal oxidation.

Chemical oxidation is a process that involves the injection of reactive chemical oxidants into groundwater and/or soil for the primary purpose of rapid contaminant. It has several advantages such as rapid treatment time and ability to treat contaminates present at high concentrations. Also, it is effective on a diverse group of contaminates. However, it has some disadvantages such high capital and operating costs. Also, the oxidation process is sometimes non-selective where oxidants will react with other substances in the wastewater.

Thermal oxidation results in combustion of organic solids to form carbon dioxide and water. It has some advantages such as complete stabilization process to destroy all volatile solids. Also, there is no need to have pre-stabilization process and handling grease and scum. However, it has disadvantage being costly where high quantity of ash is produced without having reuse program.

Although these methods are effective to treat and remove the subject pollutants from wastewater, they suffer from such shortcoming as high cost, incompleteness of purification, formation of hazardous by-product, and applicability to only concentration range [3].

Adsorption, on the other hand, is considered one of the powerful treatment processes to remove VOCs from wastewater with a low cost. Also, it is considered superior method compared to other traditional treatment methods due to its simplicity, high efficiency, ease of operation and ability to treat pollutants in more concerned forms. It is a mass transfer process that involves contact of a solid (adsorbent) with a fluid contacting the target solute (adsorbate). The surface area of the adsorbent generally governs adsorption efficiently and selectivity as a result of accumulating of the adsorbate on the surface of the adsorbent.

The adsorbent materials are classified into three categories:

1. Oxygen containing compounds which are hydrophilic and polar in nature. Examples of these materials are silica gel and zeolites.

2. Polymer based compounds. These compounds are either polar or non-polar functional groups in a porous polymer matrix such as resin.

3. Carbon based compounds which are hydrophobic and non-polar, including materials such as activated carbon.

Despite the fact that the above adsorbents are efficient in removing solutes from aqueous solution, activated carbon is considered the best one due to its large surface area and pore size distribution.

The uses of carbonaceous materials as adsorbent, in general, dates back to the prehistoric Egyptians were they used to treat water with this material. By 1901, scientists had developed ways to synthesize activated carbon from coal that had equivalent or superior adsorptive and decolorizing capacity to bone black. These adsorbents were soon introduced to the united states in 1911 for removal of taste and odor from municipal water (Burdock, 1997) [4].

The wide uses of activated carbon as adsorbent for the removal of different variety of pollutants from wastewater is due to its high adsorption capacity, fast adsorption kinetics and ease of regeneration. This is attributed to the high surface area, microporous structure and special reactivity. Another advantage of using activated carbon is that it can be produced from large raw materials that are handy and available.

The prices of commercially available activated carbons are relatively high and hence, limit their usage. Therefore, this has prompted a growing research interest in the production of activated carbons from low-costs precursors that are mainly industrial and agricultural by products. Also, the production of activated carbon from residuals may allow waste products to offset their increasing waste disposal cost against the cost of carbon production, while saving non-renewable natural resources and producing a valuable product with potential applications in pollution control.

There are many natural sources for activated carbon synthesis such as oil palm fiber, rice straw, pecan shell, corn cobs and palm seeds. Most of these materials contain functional groups associated with proteins and cellulose as major constituents.

Saudi Arabia is considered among the largest producers of dates. Dates reached an annual production of 568,000 tons in 1996, making the kingdom one of the world's largest producer of dates with 13 million date palms under cultivation. The dates production has increased to 620,000 tons in year 2000 and is expected to be more that 800,000 by year 2008 (The_Saudi_Network, 2005) [5]. Therefore, large date's stone will be expected to be produced without beneficial use.

1.1 Syntheses of Activated Carbon

The basic processes for manufacturing activated carbon involve the individual or combination of steps; Chemical and Physical activation.

In chemical activation, stage called (Wet Oxidation) the raw material is impregnated with an activation reagent such as $ZnCl_2$, HNO_3, H_2SO_4 and H_3PO_4, and heated in an inert atmosphere. The purpose is to increase the formation of functional groups without the damage of the fiber surface. Physical activation (Dry Oxidation) process normally involves two stages, hydrolysis (also called carbonization) and activation. In the first stage, the starting materials are pyrolyzed at a moderate temperature (700-900 ^{o}C) to remove the volatile matters and produce chars with basic pore structures. Subsequently, in the second stage, the resulting chars are subjected to a partial gasification at a higher temperature (usually > 900 ^{o}C) with oxidizing carrier gas or water vapor. Such materials are steam, carbon dioxide, air or a mixture of these. The final product is a well-developed structure and has an accessible internal porosity. These also can de-carboxylate the activated carbon by reducing the number of functional groups and enhancing hydrophobicity.

1.2 Objective

The purpose of this research was to prepare activated carbon from local palm seeds utilizing both activation methods chemical and physical. Moreover, the use of agricultural wastes will solve the impact of accumulation of this byproduct in environment and will reduce the manufacturing cost of activated carbon. It is expected that chemical activation treatment will open several macropore in the carbon structure and increase the surface area. This will reduce the physical activation temperature and hence reduces the energy cost for producing activated carbon. The purpose was to have activated carbon with high surface area and low manufacturing cost.

The resulted activated carbon was characterized and analyzed according to Brunauer-Emmett-Teller (BET) pore distribution, Zero point of charge (ZPC), Scanning Electron Microscope (SEM) and Fourier Transform Infrared Spectroscopy (FTIR).

The resulting highest BET surface area was utilized to remove 4-chlorophenol from wastewater. Various kinetic parameters for adsorption of these pollutants such as effect of adsorbent (activated carbon) mass, effect of adsorbate (pollutant) solution's pH, effect of adsorbate solution's concentration and effect of adsorbate solution's temperature were studied.

The literature pertaining in this thesis is presented in chapter 2. Chapter 3 illustrates the experimental procedures and apparatus, while chapter 4 provides the results and discussion. Finally conclusions and recommendations are reported in chapter 5.

CHAPTER 2

2. LITERATURE REVIEW

Several studies were conducted to synthesize activated carbon from agricultural wastes and other sources and used it for different applications of removing pollutants and contaminates. Various materials were utilized as raw material for preparing activated carbon these materials include sapropelitic coal, olive stone, coconut shell, fruit stone, surplus sewage sludge, waste tires, coffee ground, pecan shell, honeycomb, apricot stone , oil shale tendu leaf and palm seeds.

The prepared activated carbons were utilized to remove organic and nonorganic contaminants from wastewater. These contaminates include nickel (II) , methylene blue, basic dye, argon, cadmium Cd (II), lead Pb (II), chromium Cr (II), phenol, benzene , toluene , xylene mercury and 4-chlorophenol. Several research efforts were conducted to produce activated carbon with high surface area and affinity for solutes removal from wastewater.

Shawabkeh et al. prepared a novel activated carbon from pecan shells. The raw material was impregnated with phosphoric acid solution and air was injected into reaction mixture during activation for enhancing the pore size distribution and opening more surface area. Then, the activated carbon was washed by water and followed by sodium hydroxide treatment. The new activated carbon was characterized for surface area and used for strontium and copper adsorption from aqueous solution [6].

Shawabkeh et al. prepared activated carbon from spent lubrication oil by chemical activation using sulfuric and nitric acid solutions. The resulted activated carbon's functional groups were analyzed using FTIR. The analysis showed the presence of several functional groups on the surface of this activated carbon such phenolic, lactonic. The activated carbon was used to adsorb lead and cadmium from aqueous solution [**7**].

Zboon et al. prepared activated carbon from asphalt using sulfuric acid to obtain a mixture with different weight rations of acid/asphalt ranging from 20:1 to 60:1. Then, the mixture was agitated vigorously at temperature values ranging from 450 to 900 ^{o}C, while compressed air was sparged throughout the solution. The yield was affected with increasing acid/ asphalt weight ration or air flow. Also, cation exchange capacity (CEC) was found to increase with increasing airflow and temperature [8].

Hu and Vansant prepared a novel activated carbon via activating elutrilithe with potassium hydroxide (KOH). The surface area and total pore volume of the activated carbon were estimated using nitrogen adsorption isotherm at 77 K. The surface area of the new activated carbon was 112 m^2/g and total pore volume was 0.589 cm^3/g. Then, it was used for benzene, toluene and xylene adsorption [9].

Hasar synthesized activated carbon from almond husk using sulfuric acid. The resulted activated carbon was used to adsorb nickel (II) ions from aqueous solution. Also, several conditions affecting adsorption processes were investigated such pH, contact time, initial concentration of metal ions and adsorbate concentration. The experiment showed that optimal conditions for Ni

(II) removal are at 700 ^{o}C through the addition of H_2SO_4, pH of 5.0, 50 minutes of contact time and 5.0 g/liter of adsorbate concentration [10].

Yang and Lau prepared activated carbon from pistachio-nut shells utilizing potassium hydroxide (KOH) as chemical oxidizing activation agent. The experimental results showed that carbon porosity depends on the preparation conditions such as chemical impregnation ratio; activation temperature and activation hold time. The optimal conditions for preparing activated carbons with high surface area and pore volume are at impregnation ratio of 0.5, 3 hours activation time and 800 ^{o}C activation temperature. With previous optimal conditions, the obtained BET surface area and total pore volume were 2259.4 m^2/g and 1.10 cm^3/g respectively [11].

Bansode et al. prepared activated carbon from pecan shell using phosphoric acid as chemical agent and carbon dioxide as physical activation agents. The activated carbon was used for metal ions removal of (Cu^{2+}, Pb^{2+} and Zn^{2+}) from industrial wastewater. Also, the prepared carbon was compared to another commercial activated carbon used for metal ions adsorption. The experimental results showed that acid-activated carbon pecan shell adsorbed more lead and zinc ions than the commercial one. Also, the results showed that acid- and steam activated pecan shell are effective metal ions adsorbents and they can replace the commercial activated carbon [12].

Shawabkeh prepared three activated carbons from oil shale by using 95 wt. % sulfuric acid and 5 wt.% nitric acid. They were used for methylene blue adsorption at pH 7. The obtained specific surface areas for the activated carbons were 180 m^2/g, 314 m^2/g, and 292 m^2/g and total functional groups of these three samples were measured using Boehm's titration method [13].

Kobya et al. prepared activated carbon from apricot stones by impregnating it in sulfuric acid at 200 ^{o}C for 24 hours. The ability of the subject activated carbon to remove Ni (II), Co (II), Cd (II), Cu (II), Pb (II), Cr (III)x and Cr (VI) ions from aqueous solution by adsorption were investigated. Batch studies were conducted to observe the effect of pH (1-6) on the activated carbon. The higher obtained surface area was 642 m^2/g. Also, the experimental results showed that, the adsorption of these metals were found to be dependent on solution pH. The highest adsorption occurred at 1-2 for Cr (VI) and 3-6 for the rest of the metal ions [14].

Haimour and Emeish prepared activated carbon from date stones by chemical activation using both phosphoric acid H_3PO_4 and zinc chloride $ZnCl_2$ .It was observed that, iodine number increases significantly with increasing activation temperature. Also, an oscillation in the value of the iodine number noticed with increasing impregnation ratio at the same temperature. The iodine number for phosphoric acid activated carbon was higher than that for zinc chloride while the yield for H_3PO_4 was lower than that of zinc chloride. Also, it was observed that the yield decreased by increasing particle size and this is attributed to the low-porosity compact cellular structure of date stones, high viscosity and low diffusion coefficient of H_3PO_4 through the particle [15].

Bouehelta et al. prepared activated carbon from Algerian date stones by pyrolysis activation at different temperatures 500, 600, 700, and 800 ^{o}C by using 100 cm^3/min nitrogen flow and heating rate 10 ^{o}C/min. Also, the activation stage was done at 500,600,700 and 800 ^{o}C for 0.5, 1, 2, 3 or 6 hours under a nitrogen flow (100 cm^3/min) in steam. Several techniques were utilized to study the properties of the activated carbon such as X-ray diffraction (XRD), nitrogen adsorption

(BET) and FTIR. The results showed the presence of cellulose and hemicelluloses in the raw material and predominance of carbon and graphite after pyrolysis. Also, it was found aromatic structures were developed after pyrolysis and activation. The highest obtained specific surface area was 635 m^2/g at 700 ^oC under 100 cm^3/min nitrogen flow and under water vapor at 700 ^oC for 6 hours. It was found that porosity increases gradually with increasing hold time and temperature [16].

Hamed prepared activated carbon from date stones by using zinc chloride. The activated carbon was used for phenol and methylene blue (MB) adsorption. Using MB as adsorbate, it was found the optimum ratio of activator to date stone ratio (R) was 2 and the maximum unit capacity was 148 mg/g. Also, using phenol as adsorbate, it was found that the optimum R is 0.5 and the maximum unit capacity was 19 mg/g. The activated carbon produced in this study was better than that produced using H_3PO_4 as activator due to the higher capacity for activated carbon produced with $ZnCl_2$ activator [17].

Merzougui and Addom prepared activated carbon from date pits using Zinc chloride ($ZnCl_2$) and potassium hydroxide (KOH) as chemical activation agents. KOH activation produced microporosity more than $ZnCl_2$ while the last led to develop the microporisity more than KOH activation. The activated carbon was used for phenolic compounds adsorption from aqueous solution. There were three samples of activated carbons tested in this test, DC (pyrolyzed at 873 K), DK (impregnated in KOH and pyrolyzed at 1073 K) and DZ (impregenated in $ZnCl_2$ and pyrolyzed 873 K). The nitrogen surface areas are 640, 882 and 1032 m^2/g respectively. The modification of the porous texture and the surface of activated carbons were realized after

oxidation by nitric acid. The oxidation led to a decrease in the surface area, increase of the acidic functions and consequently a decrease in the capacity of adsorption of phenolic compound. Also, it was found that heat treatment of the oxidized activated carbons decreased acidic functions and increased the adsorption capacity of the activated carbon. The thermal treatment decreased the content of oxygenated functions which decreased the access of the molecules to the surface of activated carbon [18].

Alvarez et al. investigated the carbonization of activated carbon made from olive stone utilizing X-Ray scattering. The investigation's results discovered that carbonization of a lignocellulosic material such as olive stone produces large losses of carbon, oxygen and hydrogen especially up to 600 ^{o}C. The change is related to the changes in bulk density and creation of porosity [19].

Jia and Thomas studied the adsorption of cadmium ions on oxygen surface sites in activated carbon. The activated carbon was prepared from coconut shell and chemically activated using nitric acid. Various types of oxygen functional groups were introduced to the surface of the activated carbon. Fourier-Transform Infrared Spectroscopy (FTIR) and Temperature Programmed Desorption (TPD) were used to characterize the surface oxidation functional groups. The adsorption of cadmium was enhanced dramatically by oxidation of the carbon. After heat treatment of the oxidized carbons to remove oxygen functional groups, the ratio of H^{+} released to Cd^{2+} adsorbed and the adsorption capacity decreased significantly [20].

Malik et al. investigated the characterization of novel modified activated carbons for lead (II) and copper (II) adsorption from near – neutral aqueous solutions. Fruit stone was used as raw

material. Chemical activation was done using nitric acid (HNO_3) as activation and steam as physical activation agent. The carbonization was conducted at 350-700 ^oC and activation stage was carried out at 800-850 ^oC. It was found that, oxidation utilizing nitric acid results in a higher concentration of carboxylic groups [1].

Strelko et al. (2000) studied the surface reactivity and functional group content of a series of oxidized activated carbons. Different techniques were utilized to study these activated carbons such as elemental analysis and potentiometric titrations. Oxidation with hot air resulted in a greater proportion of relatively weak acidic surface functional groups (i.e., phenolic) while nitric acid modification produced a greater amount of carboxylic groups. However, by choosing a suitable modification technique, the quantities of heteroatoms (functional groups) on the surface of the active carbon can be controlled. Finally, the relatively high amount of the carbons is expected to influence the sorption capacity and selectivity of removal sorption of different ionic species from solution [21].

Martin et al. studied dyes removal from dilute aqueous solutions using activated carbon. The carbon was developed from surplus sewage sludge. It was physically activated at 700 ^oC and a rate 15 ^oC/min in nitrogen presence and held for 30 minutes. Next, it was chemically activated by sulfuric acid. The obtained new activated carbon was mainly mesoporous with a surface area of 253 m^2/g and an average pore diameter of 2.3 nm. The new activated carbon is mainly mesoporous in nature and acidic in character while the conventional activated carbon is microporus and hydrophobic. Finally, greater capacity of this new activated carbon compared to the conventional one in removing dyes from solution is attributed to its wider pore size distribution [22].

Hamadi et al. studied the adsorption kinetics for chromium (VI) removal from aqueous solution by activated carbon. The activated carbon was prepared from waste tires and used as raw material. The raw material was heated to the desired temperature (900 ^{o}C) at a heating rate of 20 ^{o}C/ min for 2 hours. Then, it was activated at the same temperature for 2 hours utilizing CO_2 as an oxidizing agent. The performance of these adsorbents against commercial activated carbon was carried out. The removal was favored at low pH, with a maximum removal at pH = 2 [23].

Jiang et al. modified the surface properties, porosities and adsorption capacities of activated carbon utilizing concentrated H_2SO_4 at temperature 150-270 ^{o}C. The modified activated carbon was used for chlorophenol, iodine, and methylene blue adsorption from wastewater and dibenzo thiophene from fuel oils. Treating activated carbon with concentrated H_2SO_4 at 250 ^{o}C increased the mesoporous volume. Also, the specific surface area had increased from 393 m^2/g to 745 m^2/g and acidic surface oxygen complexes increased too. The acidic surface oxygen groups on the modified AC increased with increasing the treatment temperatures and carboxyl's and phenols are the most abundant carbon – oxygen functional groups [24].

Yan et al. conducted a parametric study with a bench scale fixed bed to capture a traces of mercury vapor from simulated flue gas using activated carbons. Five available commercial activated carbons were tested in this experiment and several factors were investigated such as carbon loading, reaction temperature, inlet mercury concentration and particle size of the activated carbons. The experimental results showed that, the adsorption of mercury is greatly dependent upon the operation conditions. Increasing temperature will decrease physical adsorption due to the nature of exothermal adsorption process at the same time as chemisorptions might be enhanced evidenced by the better performance of carbon at a higher temperature. Also,

the external surface area of activated carbon has a significant contribution to the performance of activated carbon [25].

Mishra and Bhattacharya studied phenol removal by adsorption onto activated carbon prepared from shore a robusta leaf litter using $ZnCl_2$. The adsorption of phenol on leaf litter activated carbon follows the pore diffusion process. Also, the experimental results showed that, the rate of adsorption was affected by pH of the solution and adsorbent dosage. The maximum adsorption capacity was found in the pH range of 6-8. In addition, the carbon dose of 30 mg/L has a maximum potential to adsorb 87% phenol from its solution [26].

Girgis et al. investigated porosity development of activated carbons obtained from date pits. The date pits were chemically activated using phosphoric acid where they impregnated in phosphoric acid (H_3PO_4) with increasing concentrations (30 -70%) followed by pyrolysis at 300, 500 and 700 ^oC. Texture properties of the products were determined utilizing adsorption of nitrogen at 77 K, as well as iodine, phenol and methylene blue values. Carbon obtained at 300 ^oC was very poorly porous although it had high capacity for the uptake of iodine, phenol and methylene blue. Finally, activation with H_3PO_4 presents several advantages such as, one single thermal treatment, high carbon yield. Also, the acid is recoverable and it results in good adsorbents with mixed porosity that widens the scope of its oxidation [27].

Nemer et al. developed activated carbon from palm seeds using sulfuric acid as chemical activation agent. The carbon was used for chromium removal from aqueous solution. The experimental results showed strong dependence of the adsorption capacity on pH. The capacity increased as pH value decreased and optimal pH was found to be 1.0. The Elovich equation and

pseudo- second order equation provided the greatest accuracy for kinetic data. The study indicated that, new activated carbon from date palm seeds is an effective adsorbent for chromium removal from aqueous solution [28].

Hannafi et al. studied the modeling and optimization conditions of obtaining activated carbon form date pits. The activated carbon was utilized for phenol removal from wastewater. Several activation agents were utilized in the preparation of activated carbon. HCl, HNO_3 and H_3PO_4 acid .The effect of pH on the yield adsorption was studied in the range of 2-10. The maximum obtained adsorption was at 54 % at pH 5.5. Also, operating conditions can be optimized by optimizing stirring rate which would improve phenol elimination [29].

Shaheen et al. compared the performance of two types of activated carbons for aluminum removal from aqueous solution. The first activated carbon type was made from date- pit while the second one was commercial type. It was found that, the optimum adsorption capacities for the two adsorbents were obtained at a pH value of 4. The experimental results showed that, at low concentration region date pit activated carbon is more capable to remove aluminum than commercial activated carbon [30].

CHAPTER 3

3. EXPERIMENTAL PROCEDURES & APPARATUS

3.1 Materials & Instruments

Reagents and apparatus used in activated carbon synthesis, characterization and adsorption applications to remove 4-Chlorophenol from wastewater are listed intables 3.1 & 3.2.

Table 3.1- Regents and Chemicals Used in Activated Carbon Synthesis, Characterization & Adsorption Applications

Reagents	**Manufacturing Source**
Palm seed	Eastern Province from Saudi Arabia
Phosphoric acid, (85%)	APS Ajax Finechem Company
Carbon dioxide, (99.99%)	National Gas Company, Dammam-Saudi Arabia
Nitric acid, (69.4%)	Fisher Scientific Company
Sulfuric acid, (95.0%)	Fisher Scientific Company
De-ionized water	KFUPM Chemical Engineering Laboratories
Acetic acid glacial (99.5%)	BDH Laboratory Reagents.
4-Chlorophenol, (99+ %)	(ACROS organics)
Pellet of buffer PH=7	(BDH)
Sodium hydroxide pellets, (>99.0%)	(BDH)
Acetone (>99.0%)	Fluka

Table 3.2- Apparatus & Instruments Used in Activated Carbon Synthesis, Characterization & Adsorption Applications

Instruments	**Manufacture**
Tubular Furnace	FURNACE LINDBERG STB
Oven	FISHER ISOTEMP® Oven
Water bath	C12CS LAUDA
Atomic Adsorption Spectrometer 3100	PERKIN ELMER
De-minineralized water	ELGASTAT® UHQ
Stirrer with Hot Plate	Solid State Magnetic "9X9"
FTIR Device	16FPC FTIR PEINELMER
Spectrophotometer	UV-1601 Shimadzu
CO2 Meter	Platon
ESM Device	JEOL-JSM-6460LV
Brunauer-Emmett-Teller (BET)	Micromeritics ASAP 2010

3.2 Synthesis of Activated Carbon

Palm seeds were obtained from eastern province from Saudi Arabia as raw material for production of activated carbon. This material was chemically activated using different oxidizing agents mixed with each other at different volume ratios. After the chemical activation, the obtained activated carbon was further physically activated at different operating temperatures using carbon dioxide.

3.2.1 Raw Material Preparation

The collected palm seeds were dried at 105 ^{o}C for one day. Then it was crushed, grounded to pass 83.33 µm (180 mesh) screens and stored in closed caped flasks. All solutions were prepared using de-ionized water and all glassware was pyrex, washed with soap, and rinsed with de-ionized water before use.

3.2.2 Chemical Activation

The chemical activation was conducted utilizing different oxidizing agents with different volume ratios. These oxidizing agents are concentrated sulfuric, nitric and phosphoric acids. In a typical run, a 50 g of powdered palm seeds (particle size $\leq$ 83.33 µm) was mixed with different volume ratios of sulfuric, nitric and phosphoric acids as shown in table 3.3. The run was carried out in 3 liter beaker to obtain mixture of palm seed and acids. This mixture was heated to 160 ^{o}C with continuous stirring to have homogeneous mixture. The volume of nitric acid during the experiment was added gradually to avoid high exothermic reaction.

Table 3.3- Chemical Activation Using Different Oxidizing Agents

Exp. Name	**Palm Seed Weight (g)**	**Acid Volume (ml)**		
		H_2SO_4	**HNO_3**	**H_3PO_4**
F	50.04	0	0	200
G	50.08	0	10	190
H	50.10	0	20	180
I	50.11	0	30	170
J	50.13	100	0	100
K	50.06	66.60	66.60	66.60

During chemical activation, the palm slurry tended to change from brown to dark black color with solidification as shown in figure 3.1 . During this step, de-ionized water was added sparingly to enhance the activation and to enrich the surface functional groups of the carbon.

Once the carbonaceous material was formed, it was cooled to 22 ^{o}C and divided into two parts. The first part was equally divided into five samples and then stored in flasks for physical activation. The second part was washed several times with hot de-ionized water until the pH of supernatant reached 6.50. The washed samples were filtered, dried at 105 ^{o}C for 24 hours and stored in closed caped container for further uses.

Figure3-1: Chemical Activation Using Sulfuric and phosphoric Acids

3.2.3 Physical Activation

Generally physical activation involves two stages; hydrolysis (also called carbonization) and activation. In the first stage, the starting materials are pyrolyzed at a moderate temperature to remove the volatile matters and to produce chars with basic pore structures. Subsequently, in the second stage, the resulting chars are subjected to a partial gasification at a higher temperature (usually > 900 ^{o}C) with oxidizing gases, such as steam, carbon dioxide, air or a mixture of these, to produce final products with well-developed and accessible internal porosities.

In the presented procedure the high temperature activation was excluded were the second part of activated carbon samples prepared during the chemical activation was taken as is each sample individually and activated at certain temperature. The physical activation was carried out by taking carbonaceous material and introducing it into a quartz tube and placed inside a tubular furnace. The subject furnace was operated at various temperatures ranging from 330- 550 ^{o}C.

Then, pure carbon dioxide with a flow rate of 0.8 liter/min was introduced for 30 minutes to allow complete activation of the carbonaceous material. The obtained activated carbon was washed with de-ionized water several times until the pH of supernatant reached 6.5. The produced activated carbon was dried at 105 ^{o}C for 24 hours in an oven. Next, the samples were stored in closed caped flasks for characterization and adsorption applications. Figure 3-2 shows the experiential apparatus used in the physical activation stage. It is worth note that the sample named X in table 3.4 represents pure palm seeds powder that did not undergo chemical activation and only physical activation was applied.

Table3.4- Activation Conditions for Palm Seeds

Sample Name	**Activation Temperature (^oC)**	**CO_2 flow (Lit/min)**	**Activation Duration (minute)**
F2	330	0.80	30
G2	330	0.80	30
H2	330	0.80	30
I2	330	0.80	30
J2	330	0.80	30
K2	330	0.80	30
F1	400	0.80	30
G1	400	0.80	30
H1	400	0.80	30
I1	400	0.80	30
J1	400	0.80	30
K1	400	0.80	30
F3	450	0.80	30
G3	450	0.80	30
H3	450	0.80	30
I3	450	0.80	30
J3	450	0.80	30
K3	450	0.80	30
F4	500	0.80	30
G4	500	0.80	30
H4	500	0.80	30
I4	500	0.80	30
J4	500	0.80	30
K4	500	0.80	30
F5	550	0.80	30
G5	550	0.80	30
H5	550	0.80	30
I5	550	0.80	30
J5	550	0.80	30
K5	550	0.80	30
X1	300	0.80	30
X2	400	0.80	30
X3	450	0.80	30
X4	500	0.80	30
X5	550	0.80	30

Figure3-2: Physical Activation Using LINDBERG STB Furnace

3.3 Characterization of the Produced Activated Carbon

After using both methods of activation (chemical & physical), the produced activated carbon was characterized using different techniques to test and evaluate its properties and surface chemistry.

3.3.1 Surface Area & Pore Size Distribution

Brunauer-Emmett-Teller (BET) is adsorption technique used to measure the surface area of activated carbon. BET surface area and pore volumes for the produced activated carbon samples were both determined via Micromeritics ASAP 2020 using nitrogen adsorption at 77.35 K. A sample of 0.3210 g was degassed and dried at 150 ^{o}C for 6 hours under vacuum condition. The specific surface area and pore volume were measured and calculated by a BET equation where the cross-section area of nitrogen molecule was 0.162 nm^2.

3.3.2 Zero Point of Charge (pH_{ZPC})

The charge distribution on the carbon surface plays a major role for its adsorption affinity. When the pH of the solution is higher than pHzpc, it promotes the adsorption of positively charged ions on the surface while at a lower value it becomes more pronounced to attract negatively charged ions.

pH_{ZPC} was determined utilizing a batch equilibration technique to find the pH value at the zero point of charge. A fixed weight of 0.2g of activated carbon samples were introduced into a set of 100 ml of 0.1M KNO_3 solutions where the initial pH was adjusted from 2 to 11 by addition of either HNO_3 or NaOH. Suspended solids in the solutions were allowed to equilibrate for 24

hours in a shaker at room temperature (22±1 ^{o}C). After equilibration the final solution's pH was measured again and the difference between initial and final pH was plotted against $pH_{initial}$.

3.3.3 Scanning Electron Microscope (SEM)

Scanning electron microscope (SEM) is a type of electron microscope that images the sample surface by scanning it with a high-energy beam of electrons in a raster scan pattern. The electrons interact with the atoms that make up the sample producing signals that contain information about the sample's surface topography, composition and other properties such as electrical conductivity. Also, it shows irregular and porous surfaces. SEM analysis was conducted using a JEOL JSM-646LV Scanning Electron Microscope. The sample was initially dried, fixed with double-side masking tape, and then gold-coated using a sputtering machine for 6 minutes in order to improve the conductivity of the sample. Once the gold coating was completed, the specimens were viewed on the SEM at different magnifications.

3.3.4 Fourier Transform Infrared Spectroscopy (FTIR)

FTIR is a technique that is used to obtain an infrared spectrum of absorption, emission, photoconductivity of a solid, liquid or gas. Also, it is most useful for identifying chemicals that are either organic or inorganic and to show the surface functional groups. The functional groups on the surface of the activated carbon were analyzed using FPC FTIR Pekin Elmer spectrophotometer. A weight of 1-2 mg of the activated carbon was added to 100 mg of KBr and made into a pellet. The sample was then exposed to a laser beam from the FTIR instrument and scanned.

3.4 Adsorption Isotherm Experiments

An adsorption isotherm is a graphical representation showing the relationship between the amount adsorbed by a unit weight of adsorbent (e.g. activated carbon) and the amount of adsorbate remaining in a test medium at equilibrium [31]. It maps the distribution of adsorbate solute between the liquid and solid phases at various equilibrium concentrations. The adsorption isotherm is based on data that are specific for each system and the isotherm must be determined for every distribution. The obtained equilibrium date can be modeled using several isotherm models such as Langmuir, Freundlich and Shawabkeh Tutunji isotherm model.

The equilibrium adsorption isotherm for the adsorption of 4-chlorophneol on activated carbon surface was measured at room temperature (22 ^{o}C) and controlled pH of 6.50. The adsorbent mass was 0.1 g of activated carbon and volume of the solution was 100 ml.

3.5 Effect of pH on Adsorption Isotherm

The effect of 4-chlorphenol solutions' final pH on activated carbon surface was investigated. For 4-chlorophenol, ten samples of 200 ppm were prepared and their initial pH was varying from 2.0 to 11.0 using nitric acid and sodium hydroxide to control the pH. Then, 100 ml of the solution was put in 150 ml flasks. Next, equal weight of 0.2 g of activated carbon was added to each sample and left in shaking machine for 24 hours and then their pH values and their absorbance were measured with a purpose to measure their equilibrium concentration.

3.6 Adsorption Kinetic Studies

Several parameters affecting the adsorption processes of 4-chlorophneol were investigated. These parameters include adsorbent mass (activated carbon), pH of the solution, temperature of the solution and finally 4-chlorophenol's concentrations.

In a typical run, 85 ml of 4,000 ppm concentrated 4-chlorophenol was added to 1.7 liter of de-ionized water to get a solution of 200 ppm. The solution was mixed in a 3 liter beaker. Then, one pellet of pH 7.0 was added to the solution. The subject solution was mixed properly for five minutes using magnetic stirrer until the pH pellet dissolved completely. The purpose is to get homogenous solution. After that, the agitator was inserted inside the beaker and run at fixed rpm. After that, 3 ml of the solution was collected before adding activated carbon to the solution and considered for initial concentration measurement. Afterward, a certain weight of activated carbon sample was added to the solution. Next, a 3 ml from the solution was collected at 1, 3, 5 , 10, 15, 20, 30, 45 and 60 minutes from adding the adsorbent to the solution. Several factors impacting adsorption processes were studied and investigated. Table 3.5 shows the experimental conditions for studying the adsorption of 4-chlorophenol from wastewater.

Table 3.5- Experimental Conditions for 4-Cholorphenol Removal from Wastewater

Exp. No	**Changed Factor**	**Initial Concentration (ppm)**	**AC Mass (g)**	**Mixer Speed (rpm)**	**pH_i (Initial)**	**pH_f (Final)**	**Temp. (^oC)**
1	Concentration	200	2.0	30	7.0	6.64	22
2	Concentration	100	2.0	30	7.0	6.64	22
3	Concentration	300	2.0	30	7.0	6.64	22
4	Mass	200	2.0	30	7.0	6.64	22
5	Mass	200	1.0	30	7.0	6.64	22
6	Mass	200	3.0	30	7.0	6.64	22
7	pH	200	2.0	30	7.0	6.64	22
8	pH	200	2.0	30	4.0	3.20	22
9	pH	200	2.0	30	9.0	8.25	22
10	Temperature	200	2.0	30	7.0	6.64	22
11	Temperature	200	2.0	30	7.0	6.64	1
12	Temperature	200	2.0	30	7.0	6.64	10
13	Temperature	200	2.0	30	7.0	6.64	35
14	Temperature	200	2.0	30	7.0	6.64	50

CHAPTER 4

4. RESULTS & DISCUSSION

4.1 Synthesis and Characterization of Activated Carbon from Palm Seeds

The chemical composition of the palm seeds obtained after drying at 105 ^{o}C is shown in table 4.1. Carbohydrates and fibers are the major components of palm seeds. The seeds were activated using two different activation stages; a wet oxidation using mixed acids with different volume ratios followed by final carbonization step. In the first stage the mixture of the palm seeds and acids was heated to 160 ^{o}C where a yellowish gas was released from the reaction vessel. In the second stage the activated carbon sample was placed in a tubular furnace, and subjected to be heated to 330- 550 ^{o}C in carbon dioxide environment to open up macropores in the cellulosic structure of the palm seeds.

Table 4.1- Chemical Composition of Palm Seeds

Compound	**Content (%)**
Moisture	5-10
Protein	5-7
Oil	7-10
Crude fiber	10-20
Carbohydrates	55-65
Ash	1-2

White and brown colored gases were released from the reaction vessel which is mainly CO, CO_2, water, nitrous and phosphorous oxides. During activation the intensity of these gases is increased

with the degree of solidification of the mixture. The color of the gases changed from white to brown with the addition of more nitric acid. In this stage the cellulose within the seeds undergoes a hydrolysis reaction from the acids, where the acids attack the acetal linkages, cleaving the 1-4-glycosidic bonds. This oxidation of cellulose forms aldehyde, ketone, and carboxyl groups (Coseri et al., 2009) [32]. Increasing the degree of activation by increasing the mixture temperature evaporated the water content in the mixture leaving a highly concentrated acid distributed homogeneously around the cellulose surface. It was noticed that nitric acid reacted first with the palm sample as the intensity of the brown color was high at the beginning of the reaction and diminished with the progress of the reaction. This continued until the consumption of nitric acids left only phosphoric acid in the reaction mixture. At 160 ^{o}C phosphoric acid reacted further with the sample by extracting water molecules from cellulose structure. Consequently, this structure attained pure carbon in a lattice arrangement (Kim et al., 2001) [33]. Higher activation conditions would lead to a complete oxidation reaction converting the cellulose into CO_2 and H_2O. It was noticed that in this step pure carbon dioxide was allowed to react with the carbonized sample to yield more micropores where oxygen and hydrogen atoms separately adsorbed on neighboring sites (Long and Sykes, 1948) [34]. The oxidizing gas attacked the more readily oxidizable portion of the carbon surface, resulting in the development of the porous structure and the extensive internal surface area according to the reactions (Sricharoenchaikul et al., 2008) [35]:

$$CO_2 + C_x \rightarrow 2CO + C_{x-1}$$

$$O_2 + C_x \rightarrow 2CO + C_{x-2}$$

$$O_2 + C_x \rightarrow CO_2 + C_{x-1}$$

4.1.1 Yield

The yield is defined as the ratio of obtained mass of activated carbon produced after chemical and physical activation to that of original raw material mass. For chemical activation stage, the yield is calculated as following.

$$\text{Yield} = \frac{\left(M_{before} - M_{after}\right)}{M_{initial}}$$

M_{before}: Mass of activated carbon before washing

M_{after}: Mass of activated carbon after washing

M: Initial mass of palm seeds

Table 4.2 shows the results of yield after the addition of oxidizing agents with different molar ratios to the raw material of palm seeds.

Table 4.2- Chemical Activation Experiments & Their Yields

Exp. No	**Palm Seeds Mass (g)**	**Acids Volume (ml)**			**Yield (%)**
		H_2SO_4	**HNO_3**	**H_3PO_4**	
A	70.11	200	0	0	90.90
B	60.03	195	5	0	89.75
C	70	190	10	0	67.65
D	80.02	185	15	0	49.30
E	80.03	150	50	0	43.71
F	50.04	0	0	200	48.85
G	50.08	0	10	190	48.38
H	50.10	0	20	180	43.99
I	50.11	0	30	170	43.60
J	50.13	100	0	100	51.44
K	50.06	66.60	66.60	66.60	34.78

It is clear that as the ratio of nitric to sulfuric acid increases the yield is decreased. It is also noticed that increasing this ratio decreased the time required to complete the activation as shown in figure 4-1. Therefore, a good link may be attributed to the fact that more volatile compounds could evaporate from the mixture before conversion (Kandah et al., 2006) [36]. Also, oxidation strength of nitric acid is greater than that for sulfuric acid where oxygen to hydrogen ratio is 3:1 for nitric while it is 2:1 for sulfuric acid, which burn out the cellulose.

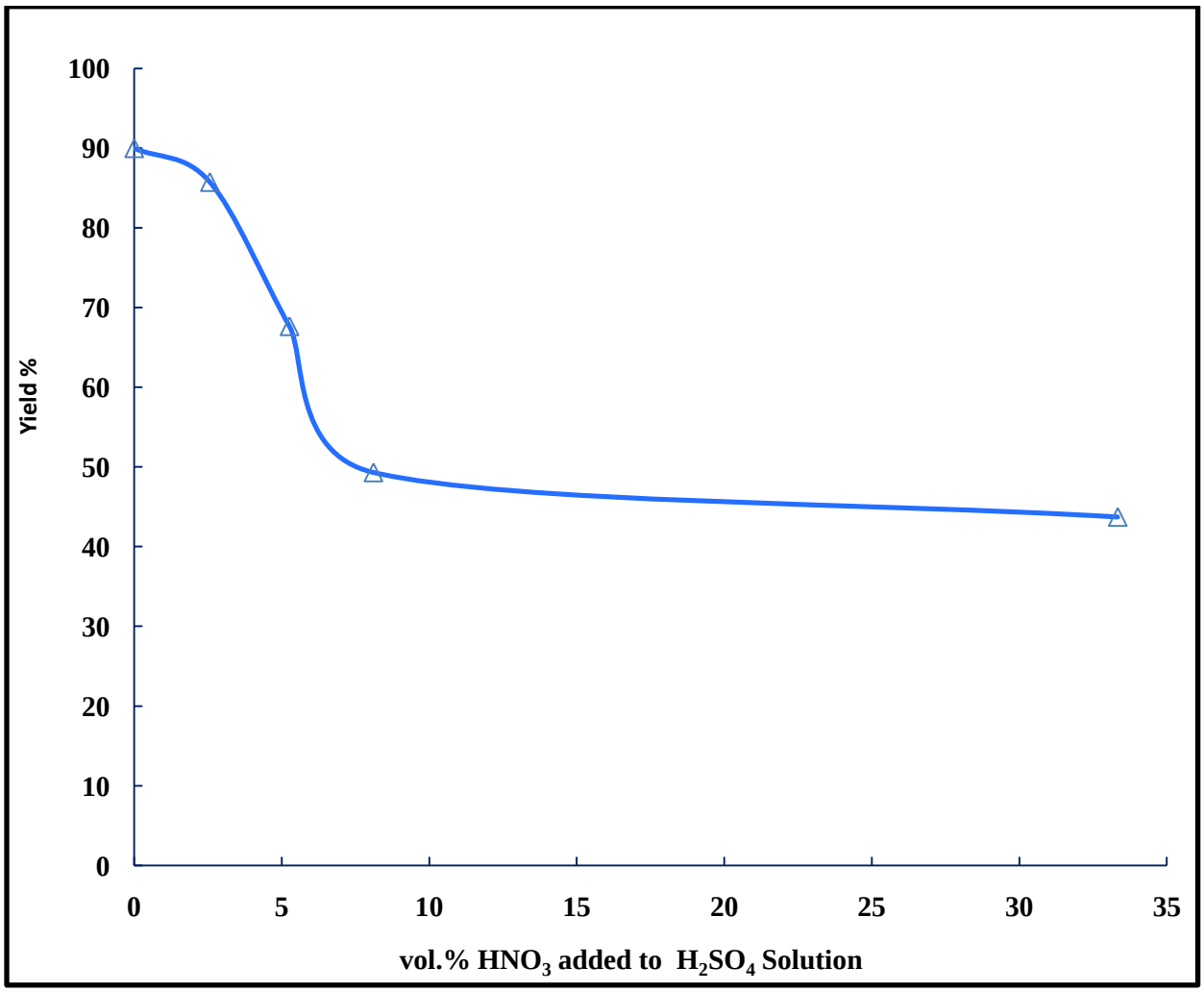

Figure 4.1- Effect of Volume Ratio of Nitric to Sulfuric Acid on Activated Carbon Yield

On the other hand, figure 4-2 illustrates the yield of activated carbon after mixing nitric acid with phosphoric acid. It is also apparent that as the ratio of nitric to phosphoric acid increases the yield decreases. This decrease is little compared to that when nitric/sulfuric mixture was used in both cases; the nitric /sulfuric acid mixture gives higher yield than that of nitric/phosphoric solution during activation.

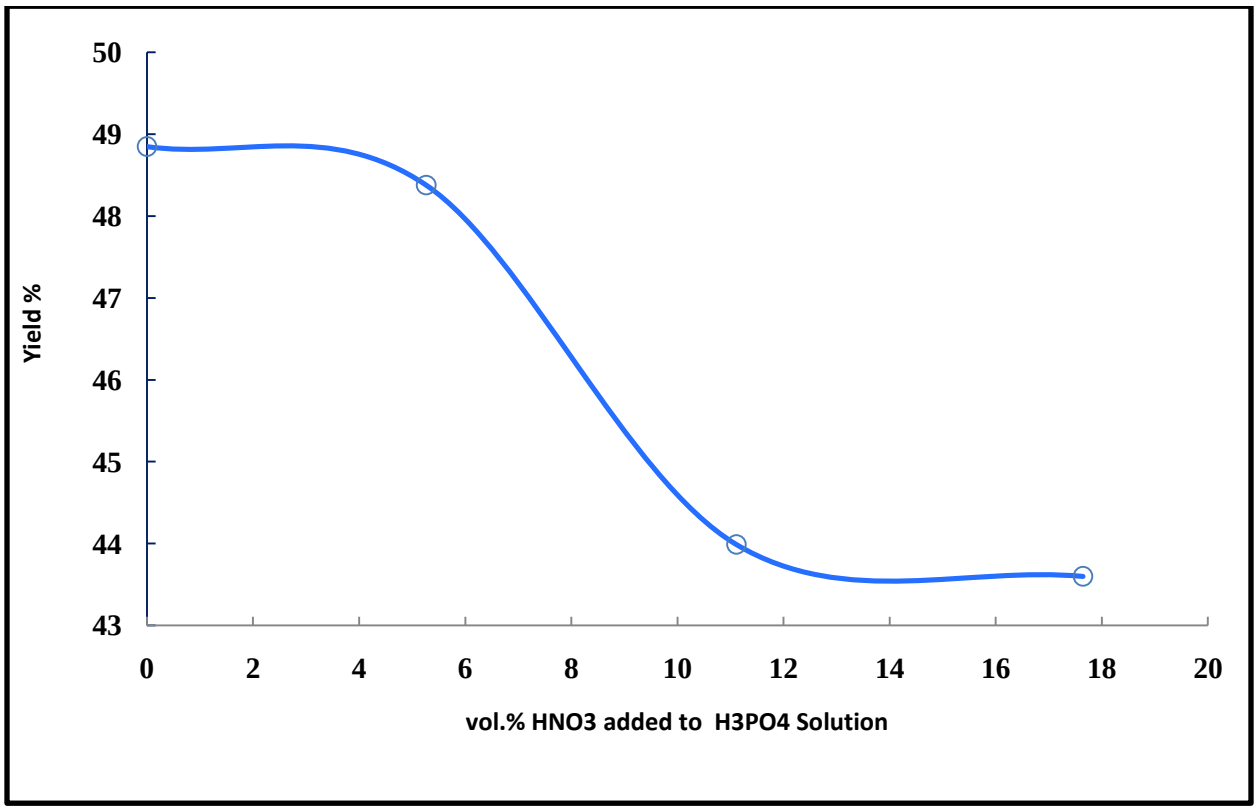

Figure 4.2- Effect of Volume Ratio of Nitric to Sulfuric Acid on Activated Carbon Yield

Table 4-2 shows that activation with pure sulfuric acid produced the highest yield of 90%, while that obtained by using only phosphoric acid produced 49%. Moreover, a mixture of 50:50 sulfuric and phosphoric acid produced a yield of 50% which indicates that phosphoric acid took over the degree of burning of the shell instead of sulfuric acid. However, the lowest yield of 34% was obtained using the mixture of the three acids (33.3 % sulfuric acid, 33.3% nitric acid & 33.3% phosphoric acid).

For physical activation, table 4.3 shows that as physical activation temperature increases the yield decreases. The reason behind this phenomenon is attributed to increasing porosity and total pore volume of the activated carbon with increasing the activation temperature. Moreover, during the physical activation the number of acidic groups' decreases and iso-electric point of the carbon is shifted to higher value. For those samples that undergo only physical activation without chemical activation, it is clear that as the activation temperature increase the yield decreases.

Table 4.3- Effect of Temperature on Yield by Physical Activation

Sample Name	**Activation Temperature (^{o}C)**	**Sample Weight (Before) Activation (g)**	**CO_2 flow (Lit/min)**	**Activation Duration (minute)**	**Sample Weight (After) Activation (g)**	**Physical Activation Yield (%)**
A2	330	65.35	0.8	30	5.37	12.27
B2	330	47.30	0.8	30	3.73	8.75
C2	330	66.17	0.8	30	5.68	6.52
D2	330	46.92	0.8	30	5.64	5.84
E2	330	68.02	0.8	30	6.54	7.40
F2	330	36.86	0.8	30	3.08	3.23
G2	330	38.18	0.8	30	3.31	3.43
H2	330	41.32	0.8	30	3.61	3.62
I2	330	39.80	0.8	30	3.59	3.58
J2	330	48.95	0.8	30	3.85	4.10
K2	330	19.97	0.8	30	2.48	3.11

Sample Name	Activation Temperature (^oC)	Sample Weight (Before) Activation (g)	CO_2 flow (Lit/min)	Activation Duration (minute)	Sample Weight (After) Activation (g)	Physical Activation Yield (%)
A1	400	55.53	0.8	30	0.8	10.40
B1	400	75.49	0.8	30	5.16	13.97
C1	400	64.48	0.8	30	5.10	6.48
D1	400	44.96	0.8	30	4.60	5.59
E1	400	34.31	0.8	30	3.61	3.73
F1	400	46.18	0.8	30	3.74	4.04
G1	400	35.73	0.8	30	3.09	3.21
H1	400	35.40	0.8	30	3.14	3.10
I1	400	44.54	0.8	30	4.01	4.00
J1	400	49.88	0.8	30	3.66	4.18
K1	400	19.73	0.8	30	2.36	3.07
A3	450	61.46	0.8	30	5.47	11.54
B3	450	61.46	0.8	30	4.39	11.37
C3	450	59.70	0.8	30	5.09	6.00
D3	450	50.94	0.8	30	2.90	6.34
E3	450	74.05	0.8	30	6.31	8.06
F3	450	47.41	0.8	30	4.00	4.15
G3	450	41.04	0.8	30	4.52	3.69
H3	450	46.50	0.8	30	4.00	4.10
I3	450	44.35	0.8	30	3.90	3.99
J3	450	48.94	0.8	30	3.76	4.10
K3	450	22.70	0.8	30	2.80	3.53
A4	500	53.45	0.8	30	4.20	10.04
B4	500	71.13	0.8	30	4.13	13.16
C4	500	38.12	0.8	30	3.22	3.83
D4	500	51.48	0.8	30	6.18	6.41
E4	500	63.24	0.8	30	6.15	6.88
F4	500	68.76	0.8	30	5.64	6.02
G4	500	52.02	0.8	30	4.63	4.68
H4	500	47.88	0.8	30	4.11	4.19
I4	500	44.11	0.8	30	3.97	3.97
J4	500	71.18	0.8	30	5.11	5.92
K4	500	26.33	0.8	30	3.20	4.09

Sample Name	Activation Temperature (^oC)	Sample Weight (Before) Activation (g)	CO_2 flow (Lit/min)	Activation Duration (minute)	Sample Weight (After) Activation (g)	Physical Activation Yield (%)
A5	550	52.91	0.8	30	4.95	9.94
B5	550	79.15	0.8	30	4.57	14.68
C5	550	74.51	0.8	30	6.72	7.48
D5	550	66.29	0.8	30	6.07	8.25
E5	550	51.51	0.8	30	5.06	5.61
F5	550	44.91	0.8	30	3.69	3.93
G5	550	52.33	0.8	30	4.28	4.70
H5	550	43.10	0.8	30	3.49	3.77
I5	550	41.91	0.8	30	3.45	3.77
J5	550	54.15	0.8	30	3.89	5.54
K5	550	23.10	0.8	30	2.64	3.59
X1	300	20.07	0.8	30	14.55	72.50
X2	400	30.03	0.8	30	15.92	53.00
X3	450	30.03	0.8	30	19.57	42.00
X4	500	30.03	0.8	30	13.76	38.00
X5	550	29.99	0.8	30	10.30	25.00

Table 4.4 shows the overall yield after both activation methods, it is clear that as the chemical yield decrease the overall yield decrease too where all experiments undergo the same physical activation temperatures.

Table 4.4 Overall Yields Resulted from Both Activation Methods.

Exp. No/ Initial Palm Seeds Mass (g)	Chemical Yield (%)	Overall Yield (%)
A (70.11 g)	**90.90**	**90.30**
B (60.03 g)	**89.75**	**89.70**
C (70.00 g)	**67.65 (3.98g)**	**73.60**
D (80.02 g)	**49.30 (7.02g)**	**54.40**
E (80.03 g)	**43.71 (3.30g)**	**49.80**
F (50.04 g)	**48.85 (3.8 g)**	**93.88**
G (50.08 g)	**48.38 (4.51 g)**	**91.46**
H (50.10 g)	**43.99 (3.27 g)**	**92.37**
I (50.11 g)	**43.6 (2.53g)**	**90.95**
J (50.13 g)	**51.46 (2.92 g)**	**85.74**
K (50.06 g)	**34.77 (2.44 g)**	**73.43**

4.1.2 Characterization of the Produced Activated Carbon

Once the carbon samples were produced, they were characterized according to their surface area, pore size distribution, surface morphology and supported functional groups.

4.1.2.1 Brunauer-Emmett-Teller (BET) Surface Area & Pore Size Distribution

The BET surface area and pore volume for activated carbon samples were determined using Micromeritics ASAP 2020 device by using nitrogen adsorption at 77.35 K. A sample of 0.3210 g was degassed and dried at 150 ^{o}C for 6 hours under vacuum. The specific surface area was measured and calculated by a BET equation where the cross-section area of nitrogen molecule

was 0.162 nm^2 (Gregg and L.Sing, 1982) [37]. It was found that the sample that treated with 200 ml phosphoric acid at 550 ^oC shows the highest surface area of 1440 m^2/g and the average pore diameter value varies between 20.69 and 24.61 Å (Table 4.4). Other values of microspores with adsorption-desorption cumulative surface area estimated by the Barrett–Joyner–Halenda (BJH) method, and Langmuir surface area are given in this table.

Table 4.5- Physical Properties of The Activated Carbon (F5) Deduced From N_2 Adsorption.

Single Point Surface Area at P/Po 0.3123	1366.66 m^2/g
BET Surface Area	1440.53 m^2/g
Langmuir Surface Area	2067.42 m^2/g
BJH Adsorption Cumulative Surface Area of Pores between 17.00 and 3000.00 Å Diameter	1032.01 m^2/g
BJH Desorption Cumulative Surface Area of Pores between 17.00 and 3000.00 Å Diameter	291.33 m^2/g
Single Point Total Pore Volume of Pores less than 3701.75 Å Diameter at P/Po 0.9947	0.745 cm^3/g
BJH Adsorption Cumulative Pore Volume of Pores between 17.00 and 3000.00 Å Diameter	0.556 cm^3/g
BJH Desorption Cumulative Pore Volume of Pores between 17.00 and 3000.00 Å Diameter	0.179 cm^3/g
Average Pore Diameter (4V/A by BET)	20.69 Å
BJH Adsorption Average Pore Diameter (4V/A)	21.54 Å
BJH Desorption Average Pore Diameter (4V/A)	24.64 Å

The pore volume distribution for this second-stage carbonized sample is shown in Figure 4.3. It is clear that the mean distribution of the pores was at *d=1* nm which provides a highly micro porous activated carbon. This pore volume distribution was modeled against Pearson's statistical model to obtain the relation between pore volume distributions, *f (γ)* and pore radius according:

$$f(r) = \frac{a_0}{\left[1 + 4\left(\frac{r - a_1}{a_2}\right)^2 \left(2^{\frac{1}{a_3}} - 1\right)\right]^{a_3}}$$

Where a_0= 0.55204, a_1= 16, a_2 = 0.9 and a_3= 1.3. The regression coefficient is 0.987 with sum of square errors 0.010.

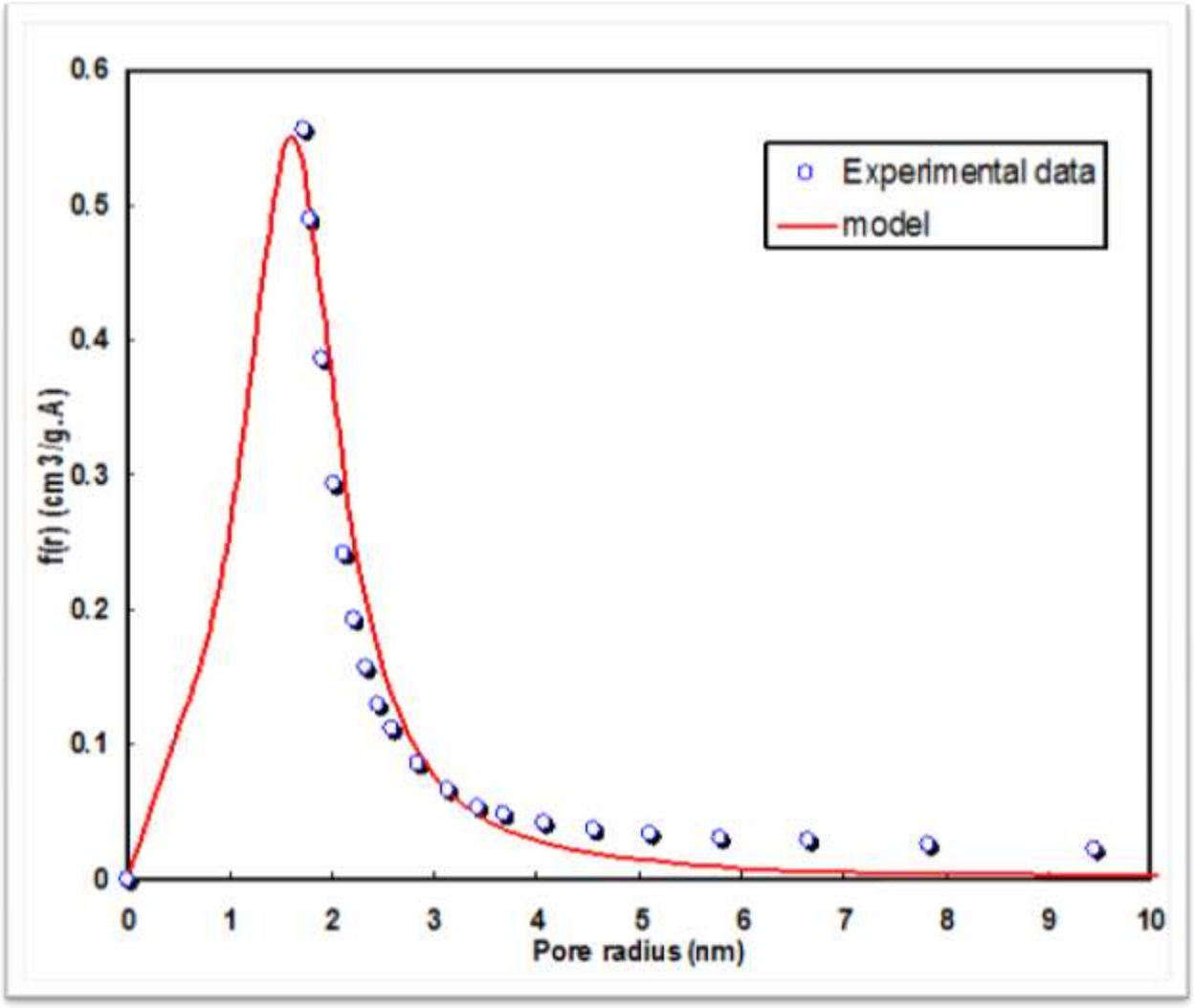

Figure 4.3- Pore Volume Distribution of Activated Carbon Sample (F5)

On the other hand, the sample that treated with equal volume ratio of phosphoric, nitric and sulfuric acids, the BET surface area was 1065.55 m^2/g and the average pore diameter value varied between 21.53 and 30.32 Å (Table 4.6). Other values of microspores with adsorption-desorption cumulative surface area estimated by the Barrett–Joyner–Halenda (BJH) method, and Langmuir surface area are given in Table 4.6.

Table 4.6- Physical properties of the activated carbon (K5) deduced from N_2 adsorption.

Single Point Surface Area at P/Po 0.3055	1014.42 m^2/g
BET Surface Area	1065.55 m^2/g
Langmuir Surface Area	1500.00 m^2/g
BJH Adsorption Cumulative Surface Area of Pores between 17.00 and 3000.00 Å Diameter	241.82 m^2/g
BJH Desorption Cumulative Surface Area of Pores between 17.00 and 3000.00 Å Diameter	190.32 m^2/g
Single Point Total Pore Volume of Pores less than 3851.58 Å Diameter at P/Po 0.9947	0.574 cm^3/g
BJH Adsorption Cumulative Pore Volume of Pores between 17.00 and 3000.00 Å Diameter	0.177 cm^3/g
BJH Desorption Cumulative Pore Volume of Pores between 17.00 and 3000.00 Å Diameter	0.144 cm^3/g
Average Pore Diameter (4V/A by BET)	21.53 Å
BJH Adsorption Average Pore Diameter (4V/A)	29.32 Å
BJH Desorption Average Pore Diameter (4V/A)	30.32 Å

For the sample that physically treated without acids, X5, the BET surface area is 1057.69 m^2/g and the average pore diameter value varies between 19.28 and 20.30 Å (Table 4.7). Other values of microspores with adsorption-desorption cumulative surface area estimated by the Barrett–Joyner–Halenda (BJH) method, and Langmuir surface area are given in Table 4.7.

Table 4.7- Physical Properties of The Activated Carbon (X5) Deduced from N_2 Adsorption.

Single Point Surface Area at P/Po 0.3055	1008.64 m^2/g
BET Surface Area	1057.69 m^2/g
Langmuir Surface Area	1479.42 m^2/g
Single Point Total Pore Volume of Pores less than 5336.32 Å Diameter at P/Po 0.9963	0.509 cm^3/g
BJH Adsorption Cumulative Pore Volume of Pores between 17.00 and 3000.00 Å Diameter	0.177 cm^3/g
Average Pore Diameter (4V/A by BET)	19.28 Å

Nevertheless, the sample that treated with nitric and phosphoric acid (30/ 70) ml/ml, the BET surface area was decreased to 976.29 m^2/g and the average pore diameter value varied between 21.31 and 23.83 Å (Table 4.8). Other values of microspores with adsorption-desorption cumulative surface area estimated by the Barrett–Joyner–Halenda (BJH) method, and Langmuir surface area are given in Table 4.8.

Table 4.8- Physical Properties of The Activated Carbon (I5) Deduced from N_2 Adsorption.

Single Point Surface Area at P/Po 0.3168	928.08 m^2/g
BET Surface Area	976.29 m^2/g
Langmuir Surface Area	1423.62 m^2/g
BJH Adsorption Cumulative Surface Area of Pores between 17.00 and 3000.00 Å Diameter	241.82 m^2/g
BJH Desorption Cumulative Surface Area of Pores between 17.00 and 3000.00 Å Diameter	614.95 m^2/g
Single Point Total Pore Volume of Pores less than 3809.65 Å Diameter at P/Po 0.9949	0.520 cm^3/g
BJH Adsorption Cumulative Pore Volume of Pores between 17.00 and 3000.00 Å Diameter	0.3488 cm^3/g
BJH Desorption Cumulative Pore Volume of Pores between 17.00 and 3000.00 Å Diameter	0.211 cm^3/g
Average Pore Diameter (4V/A by BET)	21.311 Å
BJH Adsorption Average Pore Diameter (4V/A)	22.69 Å
BJH Desorption Average Pore Diameter (4V/A)	23.83 Å

For sample that was treated with nitric/phosphoric (30 ml/ 170 ml) I6, the BET surface area was 886.57 m^2/g and the average pore diameter value varies between 20.875 and 24.496 Å (Table 4.9). Other values of microspores with adsorption-desorption cumulative surface area estimated by the Barrett–Joyner–Halenda (BJH) method, and Langmuir surface area are given in Table 4.9.

Table 4.9- Physical Properties of The Activated Carbon (I6) Deduced from N_2 Adsorption.

Single Point Surface Area at P/Po 0.3081	845.645 m^2/g
BET Surface Area	886.570 m^2/g
Langmuir Surface Area	1264.306 m^2/g
BJH Adsorption Cumulative Surface Area of Pores between 17.00 and 3000.00 Å Diameter	662.446 m^2/g
BJH Desorption Cumulative Surface Area of Pores between 17.00 and 3000.00 Å Diameter	222.468 m^2/g
Single Point Total Pore Volume of Pores less than 3809.65 Å Diameter at P/Po 0.9946	0.462 cm^3/g
BJH Adsorption Cumulative Pore Volume of Pores between 17.00 and 3000.00 Å Diameter	0.3703 cm^3/g
BJH Desorption Cumulative Pore Volume of Pores between 17.00 and 3000.00 Å Diameter	0.136 cm^3/g
Average Pore Diameter (4V/A by BET)	20.875 Å
BJH Adsorption Average Pore Diameter (4V/A)	22.361 Å
BJH Desorption Average Pore Diameter (4V/A)	224.496 Å

For sample that was treated with sulfuric/phosphoric (100 ml/100ml), J5, the BET surface area was 853.99 m^2/g and the average pore diameter value varied between 21.879 and 30.541 Å (Table 4.10). Other values of microspores with adsorption-desorption cumulative surface area estimated by the Barrett–Joyner–Halenda (BJH) method, and Langmuir surface area are given in Table 4.10.

Table 4.10- Physical Properties of The Activated Carbon (J5) Deduced from N_2 Adsorption.

Single Point Surface Area at P/Po 0.3081	812.359 m^2/g
BET Surface Area	853.999 m^2/g
Langmuir Surface Area	1210.162 m^2/g
BJH Adsorption Cumulative Surface Area of Pores between 17.00 and 3000.00 Å Diameter	703.079 m^2/g
BJH Desorption Cumulative Surface Area of Pores between 17.00 and 3000.00 Å Diameter	174.829 m^2/g
Single Point Total Pore Volume of Pores less than 4127.948 Å Diameter at P/Po 0.9953	0.467 cm^3/g
BJH Adsorption Cumulative Pore Volume of Pores between 17.00 and 3000.00 Å Diameter	0.407 cm^3/g
BJH Desorption Cumulative Pore Volume of Pores between 17.00 and 3000.00 Å Diameter	0.133 cm^3/g
Average Pore Diameter (4V/A by BET)	21.879 Å
BJH Adsorption Average Pore Diameter (4V/A)	23.186 Å
BJH Desorption Average Pore Diameter (4V/A)	30.541 Å

The decrease in surface area with adding more nitric acid resulted in the damage of some of the micropores. Moreover, higher nitric acid concentration will evaporate some of the precursor of the ash.

As the acid/palm seeds ratio increases the yield decreases. Increasing this ratio will decrease the time to complete the activation where the pores will sealed off as a result of sintering at high retention time [26]. Also, it is attributed to a sintering effect followed by the shrinkage of the

activated carbon which results in reducing the pores and finally results in reducing the surface area.

4.1.2.2 Scanning Electron Microscope (SEM)

Scanning Electron Microscope (SEM) analysis was conducted using a JEOL JSM-646LV. The sample was initially dried, fixed with double-side masking tape, and then gold-coated using a sputtering machine for 6 minutes in order to improve the conductivity of the sample. Once the gold coating was completed, the specimens were viewed on the SEM at different magnifications. SEM was conducted for three samples that showed highest surface area (F5, J5 & K5). SEM images of the carbonized sample (F5) are show in Figures 4.4:a-c. Figure 4.4-a illustrates the SEM of the activated palm samples with the emphasis on three different spectrums. Each spectrum was mainly analyzed for its carbon and oxygen content (Table 4.11). It appears that an average of 36 and 59 wt% of these spectrums has carbon and oxygen atoms, respectively. Phosphorus atoms occupied 5.8 wt% in the second spectrum which provides evidence that the carbon surface has been enriched with oxygen and phosphorus functional groups. Figures 4.4-b and 4.4 -c show the surface morphology of the activated carbon samples with high porosity where microspores were developed during activation.

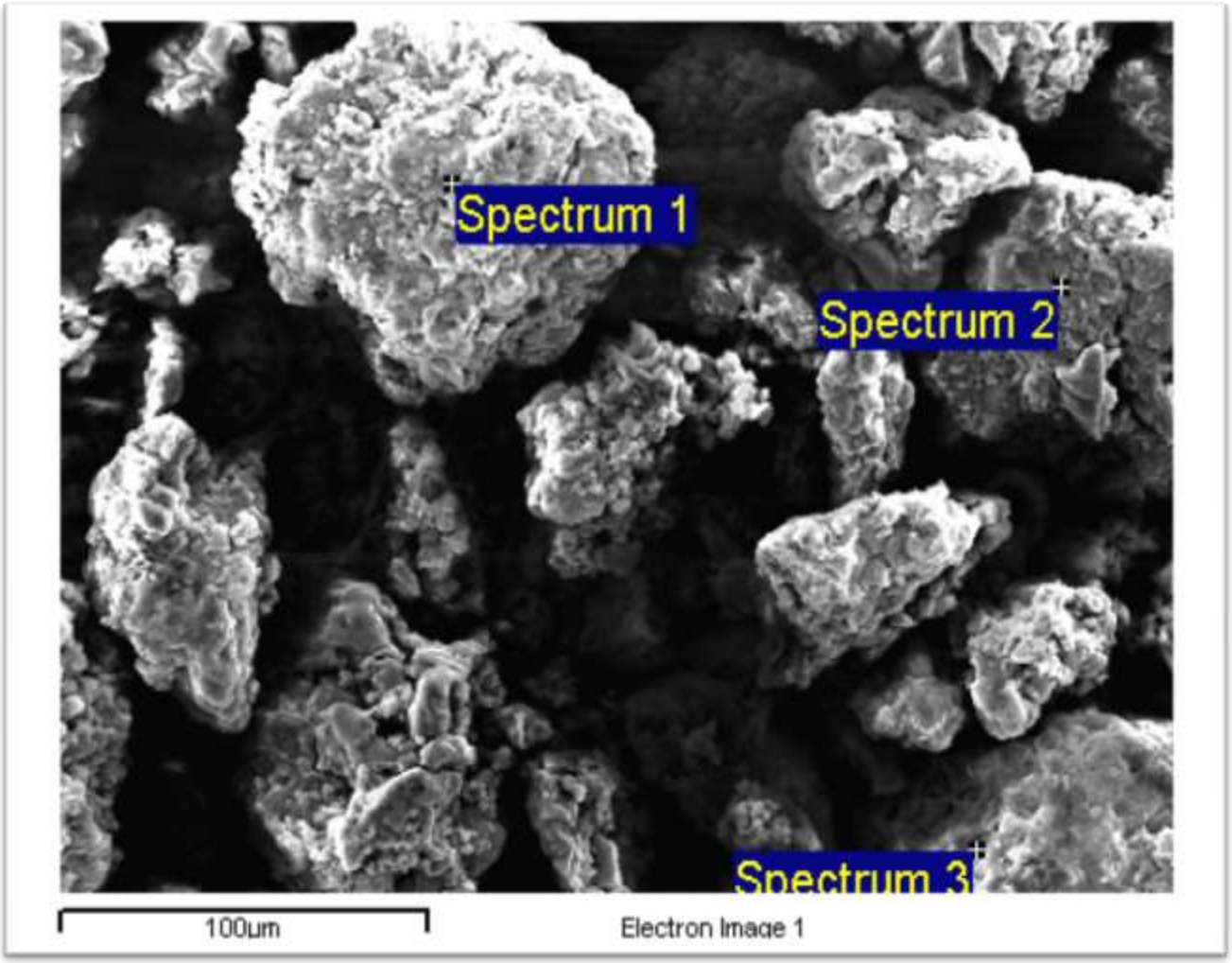

Figure 4.4.a- SEM Image for Activated Carbon Sample (F5)

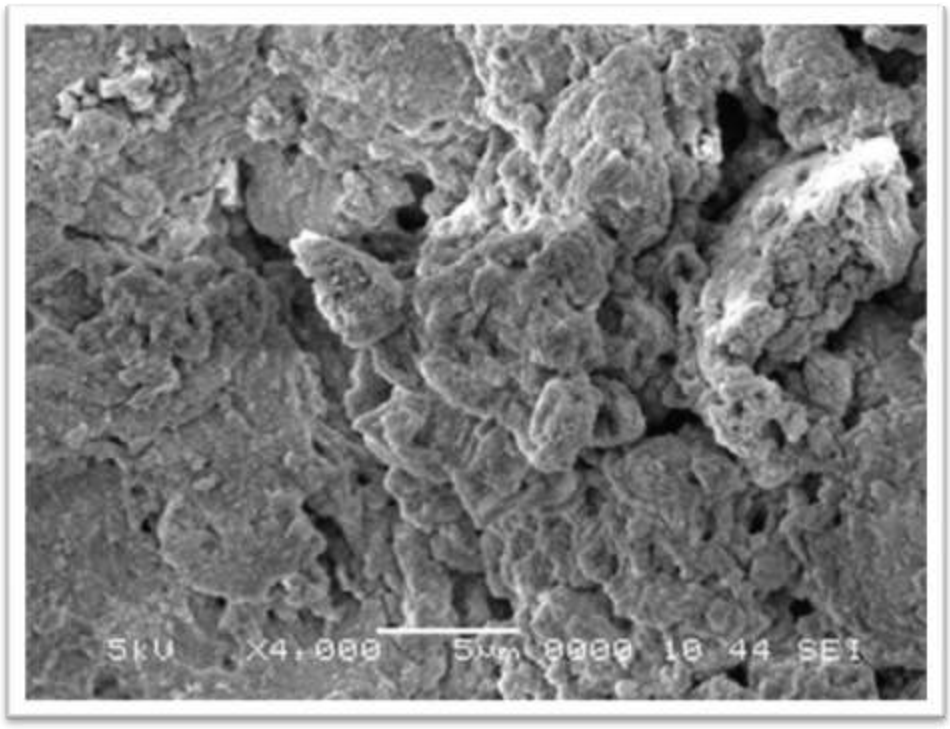

Figure 4.4.b- SEM Image for Activated Carbon Sample (F5)

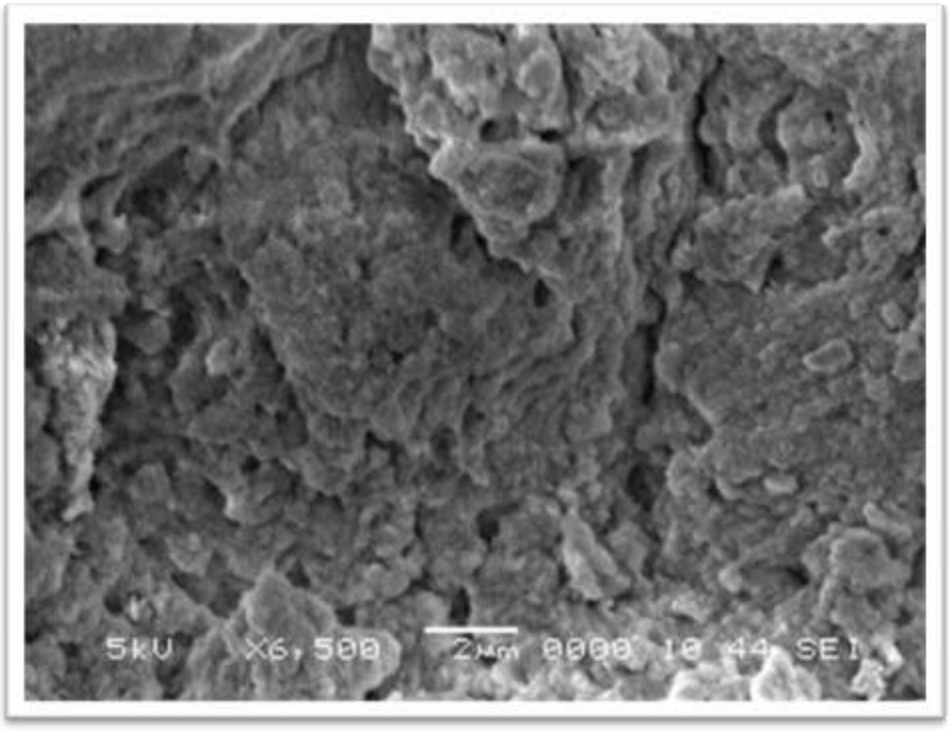

Figure 4.4.c- SEM Image for Activated Carbon Sample (F5)

Table 4.11. Normalized Element Analyses for Different Spectra of Activated Carbon (F5)

Spectrum	C (wt. %)	O (wt. %)	P (wt. %)	Ta (wt. %)	Total
Spectrum 1	44.7	51.0		4.3	100.00
Spectrum 2	34.6	59.6	5.8		100.00
Spectrum 3	30.5	67.3	1.0	1.2	100.00
Min.	30.5	51.0	0.0		

SEM images of the carbonized sample (J5) are show in Figures 4.5:a-c. Figure 4.5-a illustrates the SEM of the activated palm samples with the emphasis on three different spectrums. Each spectrum was mainly analyzed for its carbon and oxygen content (Table 4.12). It appears that an average of 21.5 and 40.2 wt% of these spectrums has carbon and oxygen atoms, respectively. Also, oxygen atoms occupied 55.4 wt% in the third spectrum. This provides evidence that the carbon surface has been enriched with oxygen functional groups by using both sulfuric and phosphoric acids. Figures 4.5-b and 4.5-c show the surface morphology of the activated carbon samples with high porosity where microspores were developed during activation.

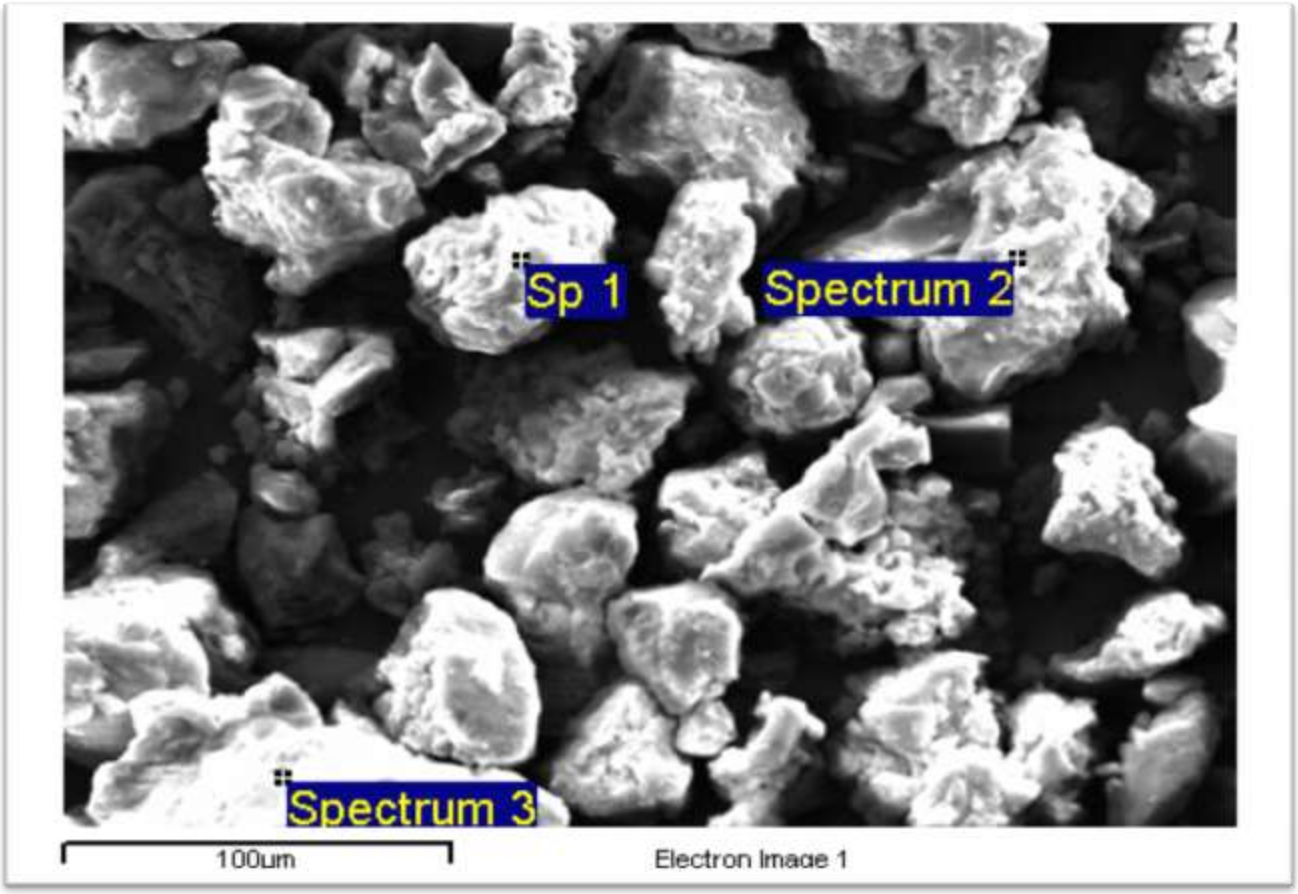

Figure 4.5.a- SEM Image for Activated Carbon Sample (J5)

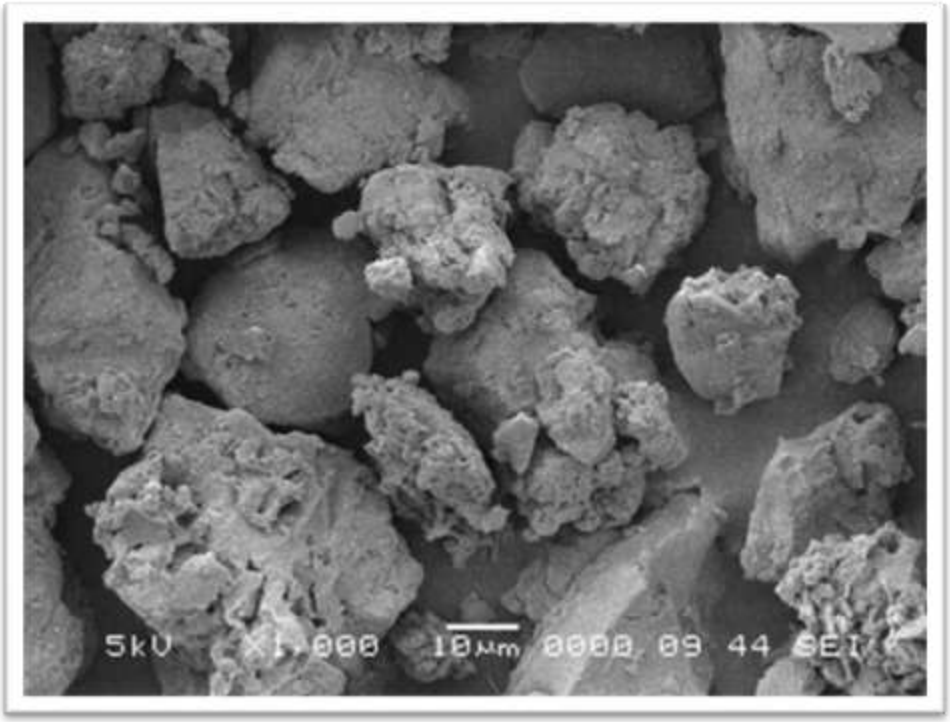

Figure 4.5.b- SEM Image for Activated Carbon Sample (J5)

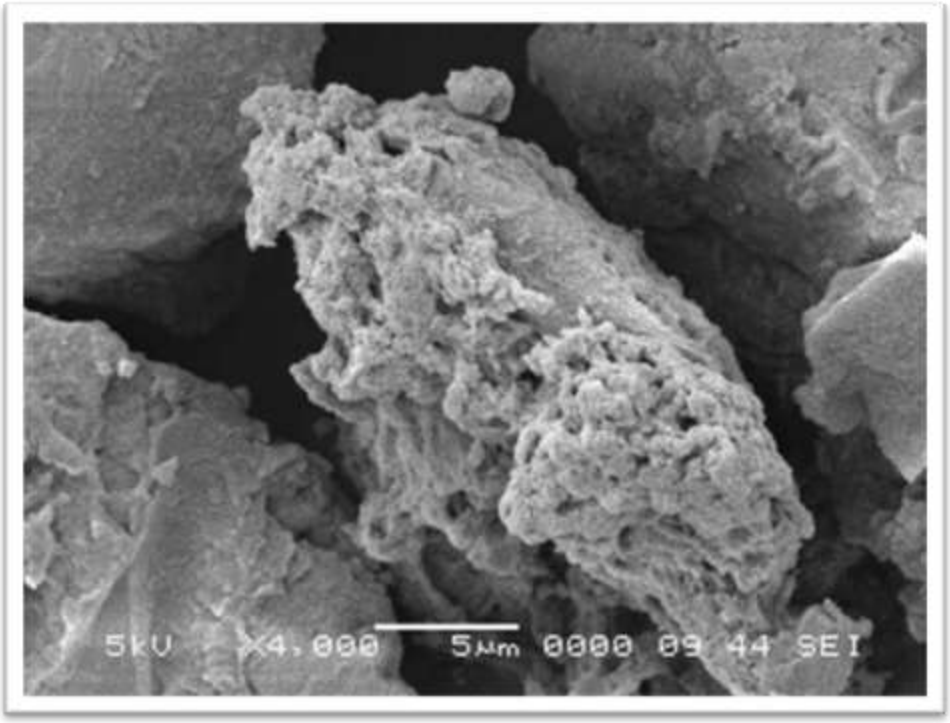

Figure 4.5.c- SEM Image for Activated Carbon Sample (J5)

Table 4.12. Normalized Element Analyses for Different Spectra of Activated Carbon (F5)

Spectrum	C (wt. %)	O (wt. %)	Cu (wt. %)	Hg (wt. %)	Total
Spectrum 1	23.80	33.36	23.56		19.28
Spectrum 2	17.03	31.75	12.88	17.44	20.90
Spectrum 3	23.86	55.38	10.47		10.29
Min.	23.86	55.38	23.56	17.44	20.90
Max	17.03	31.75	10.47	17.44	10.29

SEM images of the carbonized sample (K5) are show in Figures 4.6:a-c. Figure 4.6-a illustrates the SEM of the activated palm samples with the emphasis on three different spectrums. Each spectrum was mainly analyzed for its carbon and oxygen content (Table 4.12). It appears that an average of 22 and 46 wt% of these spectrums has carbon and oxygen atoms, respectively. Sulfur atoms occupied 1.9 wt% in the second spectrum which provides evidence that the carbon surface has been enriched with oxygen and sulfuric functional groups during the activation by three oxidizing agents (H_2SO_4, HNO_3 & H_3PO_4). Figures 4.6 shows the surface morphology of the activated carbon samples with high porosity where microspores were developed during activation.

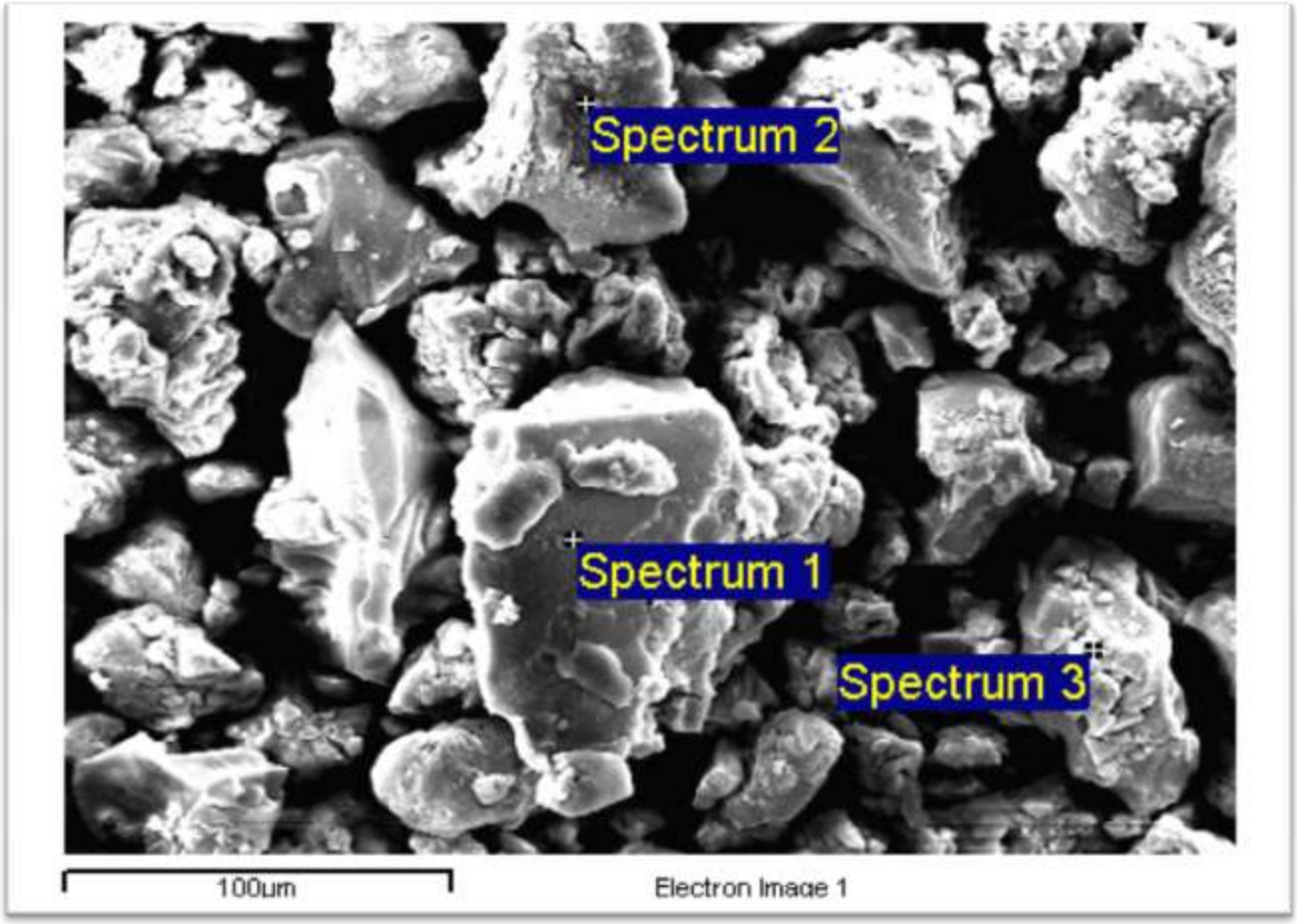

Figure 4.6.a-. SEM image for activated carbon sample (K5)

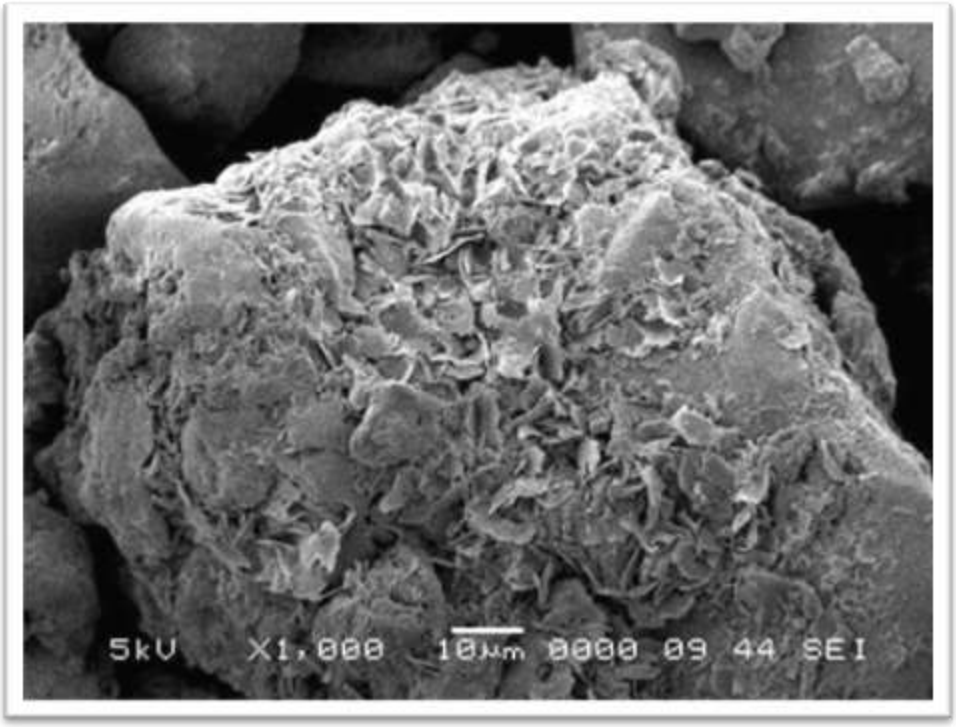

Figure 4.6.b-. SEM image for activated carbon sample (K5)

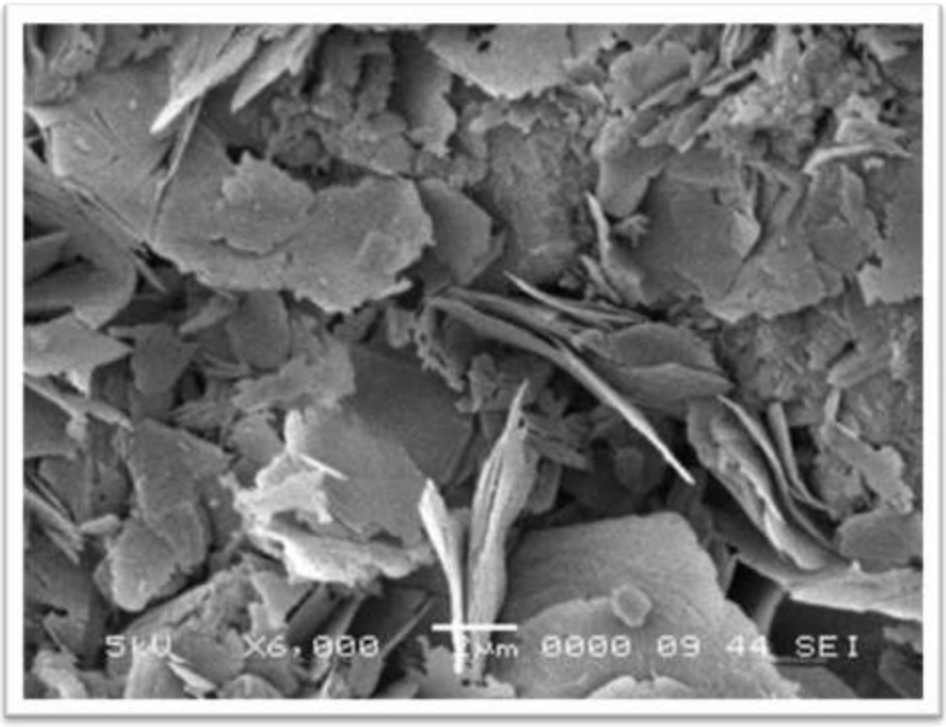

Figure 4.6.c-. SEM image for activated carbon sample (K5)

Table 4-13. Normalized Element Analyses for Different Spectra of Activated Carbon (K5)

Spectrum	C (wt. %)	O (wt. %)	S (wt. %)	Ta (wt. %)	Pt (wt. %)	Hg (wt. %)	Total
Spectrum-1	13.75	30.58			24.38	31.29	100.00
Spectrum-2	24.82	50.43	1.90		9.48	13.37	100.00
Spectrum-3	25.02	56.24	1.37	1.30	7.57	8.50	100.00
Max.	25.02	56.24	1.90	1.30	7.57	31.29	
Min.	13.75	30.58	1.37	1.30	24.38	8.50	

4.1.2.3 Zero Point of Charge (ZPC)

ZPC was determined utilizing batch equilibration technique to determine the pH value at the zero point of charge. A fixed weight of 0.2g of the activated carbon samples were introduced into a set of 100 ml of 0.1M KNO_3 solutions where the initial pH was adjusted from 2 to 11 by addition of either HNO_3 or NaOH. Suspended solids in the solutions were allowed to equilibrate for 24 hours in a shaker at room temperature (22±1 ^{o}C). After equilibration the final pH was measured again and the difference between initial and final pH was plotted against $pH_{initial}$.

Figure 4.7 shows the surface acidity of the produced carbon where the difference in solution pH before and after addition of the activated carbon to a potassium nitrate solution was measured as a function of initial solution pH. At ΔpH=0 the value of pH_{zpc} is 4.89. The charge distribution on the carbon surface plays a major role for its exchange property. When the pH of the solution is higher than pH_{pzc} it promotes the adsorption of positively charged ions on the surface while at a lower value it becomes more pronounced to attract negatively charged ions. The obtained pH_{zpc} value for this carbon indicates that there is an attractive forces between the carbon surface and cations within pH 5-7 and with anions between pH 1-5.

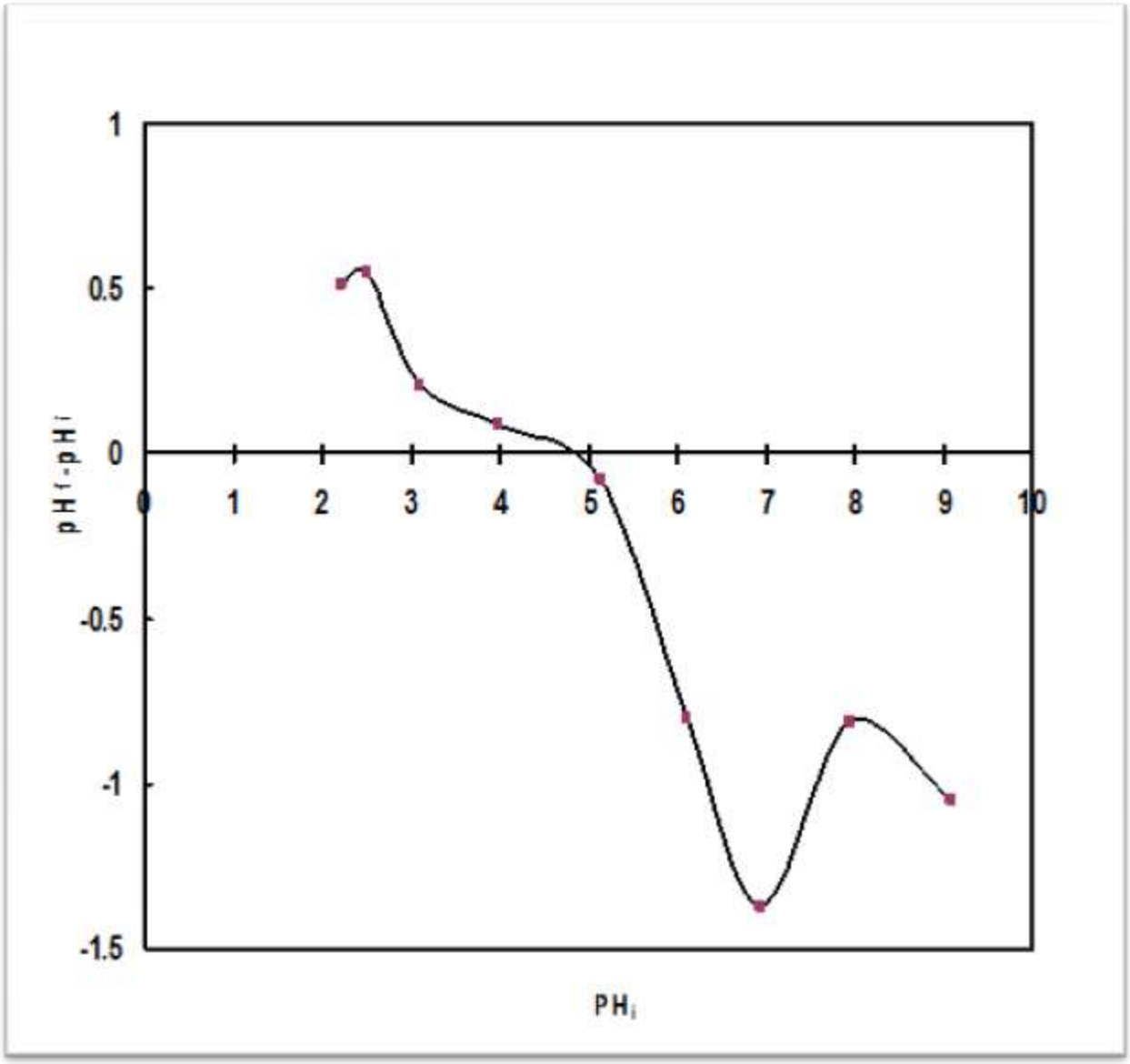

Figure 4.7- Zero point of charge for activated carbon (F5)

For sample K5, at ΔpH=0 the value of pH_{zpc} is 4.00. The charge distribution on the carbon surface plays a major role for its exchange property. When the pH of the solution is higher than pHpzc it promotes the adsorption of positively charged ions on the surface while at a lower value it becomes more pronounced to attract negatively charged ions. The obtained pH_{zpc} value for this carbon indicates that there is an attractive forces between the carbon surface and actions within pH 5-10 and with anions between pH 1-4 as shown in figure 4.8.

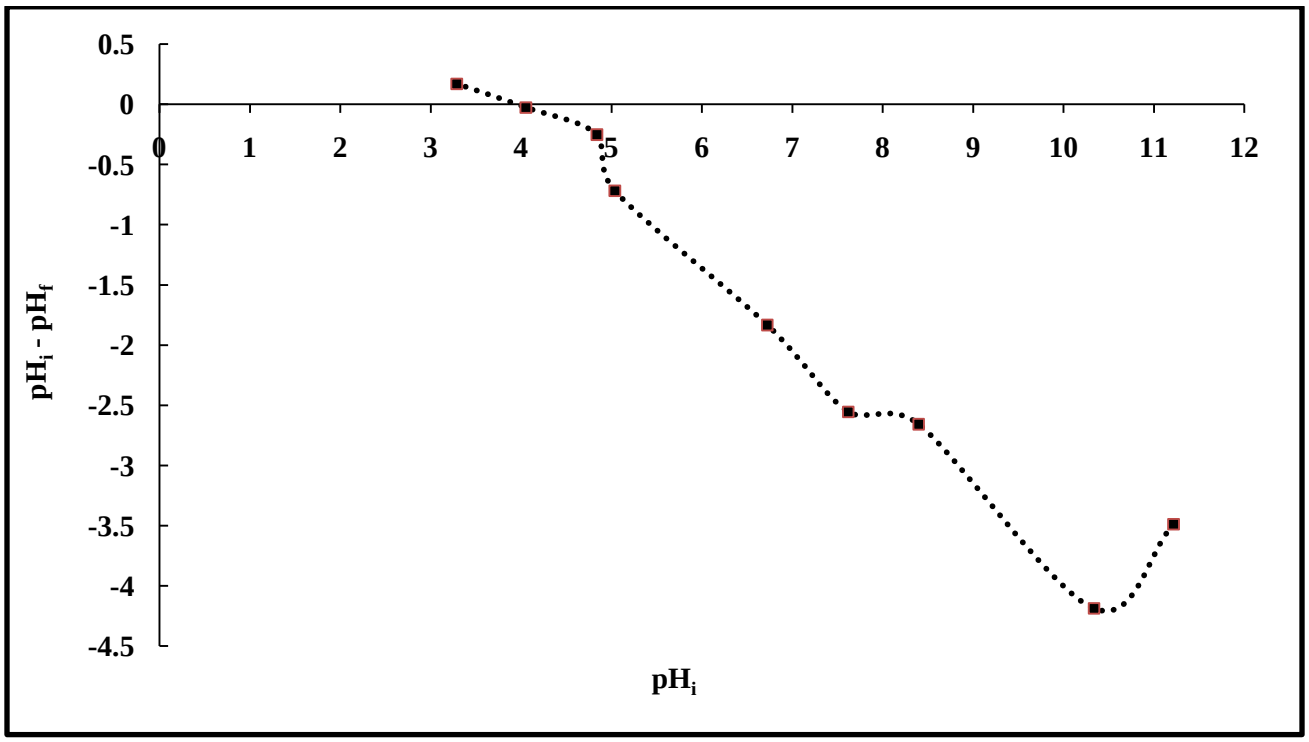

Figure 4.8- Zero POINT of Charge for Activated Carbon (K5)

For sample E5, at ΔpH=0 the value of pH_{zpc} is 3.00. The obtained pH_{zpc} value for this carbon indicates that there is an attractive forces between the carbon surface and actions within pH 3.2-7 and with anions between pH 1-3 as shown in figure 4.9.

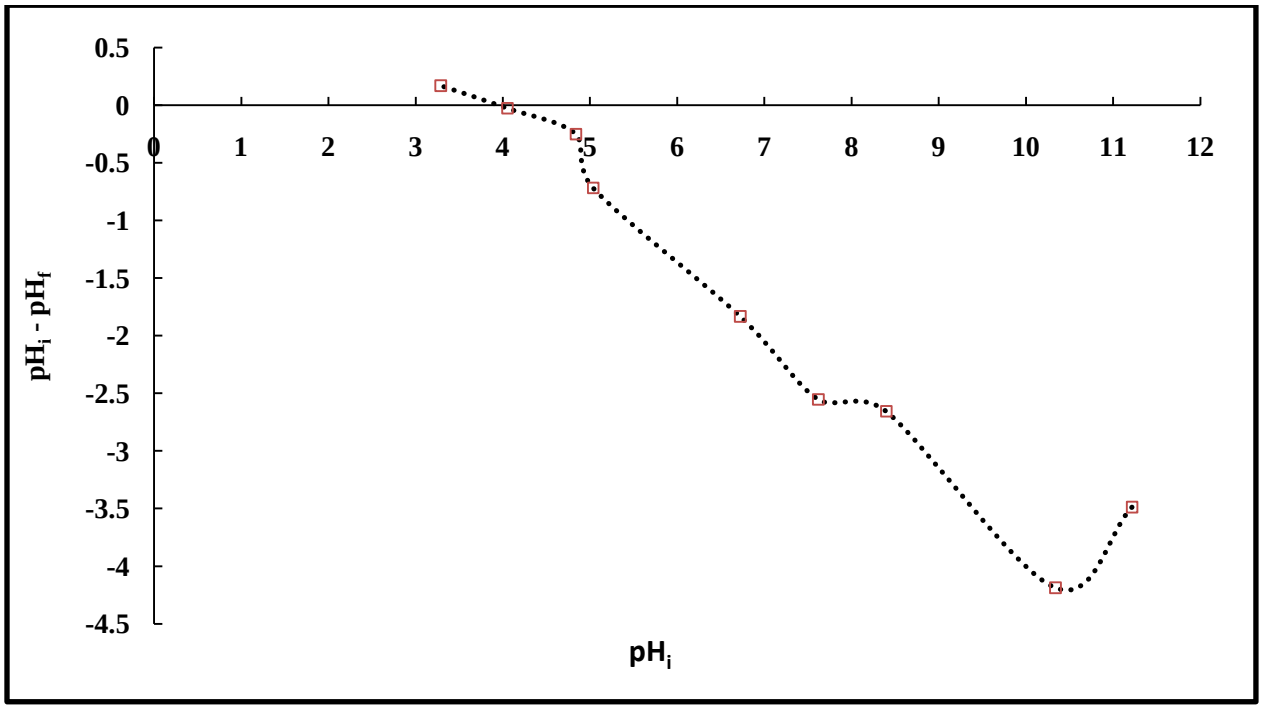

Figure 4.9- Zero Point of Charge for Activated Carbon (E5)

It is evident that all samples have close pHzpc which is attributed to the nature of palm seeds structure and intensity of the functional groups attached to the surface of produced activated carbon.

4.1.2.4 Fourier Transform Infrared Spectroscopy (FTIR)

The functional groups on the surface of the activated carbon were analyzed using FPC FTIR Perkin Elmer spectrophotometer. A weight of 1-2 mg of the activated carbon was added to 100 mg of KBr and made into a pellet. The sample was then exposed to a laser beam from the FTIR instrument and scanned.

FTIR analyses of the untreated palm seeds and of the activated ones are shown in Figure 4.10. Untreated seeds showed six distinct peaks at 3318.9, 2923.5, 2854.3, 1745.2, 1612.2 and 1039.2

cm^{-1}. The peak at 3318.9 refers to the hydrogen bond OH group of alcohols and phenol which was shifted to 3420.7 upon activation. Moreover, two new peaks, 3851.8 and 3753.1 cm^{-1}, appeared after activation which are assigned to the O-H stretching mode of hydroxyl groups and adsorbed water. The intensity of peaks 2923.5, 2854.3 in the palm seed was reduced after activation to 2920 cm^{-1} and 2834.8 cm^{-1}. These peaks are attributed to the carboxylic group (-COOH). Also a new peak at 2372.0 cm^{-1} appeared after activation which is attributed to the presence of (C≡C) group. On the other hand, the peaks at 1684.6-1745.2 cm^{-1} are related to ketone group. The intensity of the peak at 1612.2 increased and shifted to 1606.2 which is related to the presence of aromatic functional groups on the surface of activated carbon. The peak between 1155.1 and 1039.4 in the seeds became broader after activation and shifted to 1169.4 and 1057.2cm^{-1}. These peaks are attributed to the presence of (C-C) and (CO) groups on the surface.

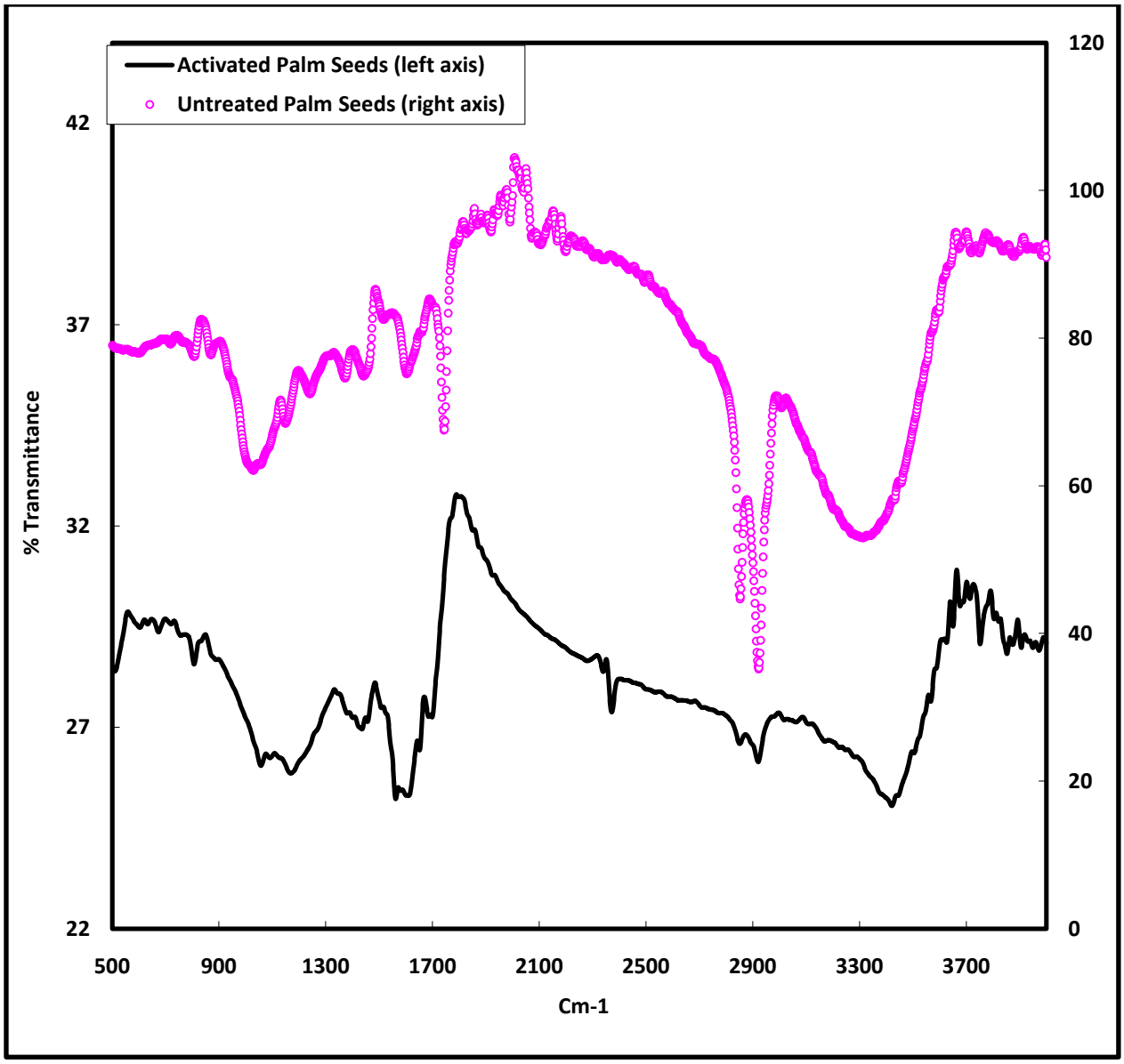

Figure 4.10- FTIR Spectrum for The Palm Seeds and Activated Carbon (F5)

FTIR analyses the activated carbon (J5) is shown in Figure 4.11. Two peaks at 3853.3 and 3754.0 cm^{-1}, appeared after activation which are assigned to the O-H stretching mode of hydroxyl groups and adsorbed water. Also a new peak at 2372.0 cm^{-1} appeared after activation which is attributed to the presence of (C≡C) group. On the other hand, the peaks at 1684.6-1700.6 cm^{-1} are related to ketone group. The intensity of the peak at 1561.7 is referred to amide

band. The peak at 1167.7 cm^{-1} is related to (C-C) and (C-O) group after the activation. The peak at 4357 cm^{-1} is referred to (C-C).

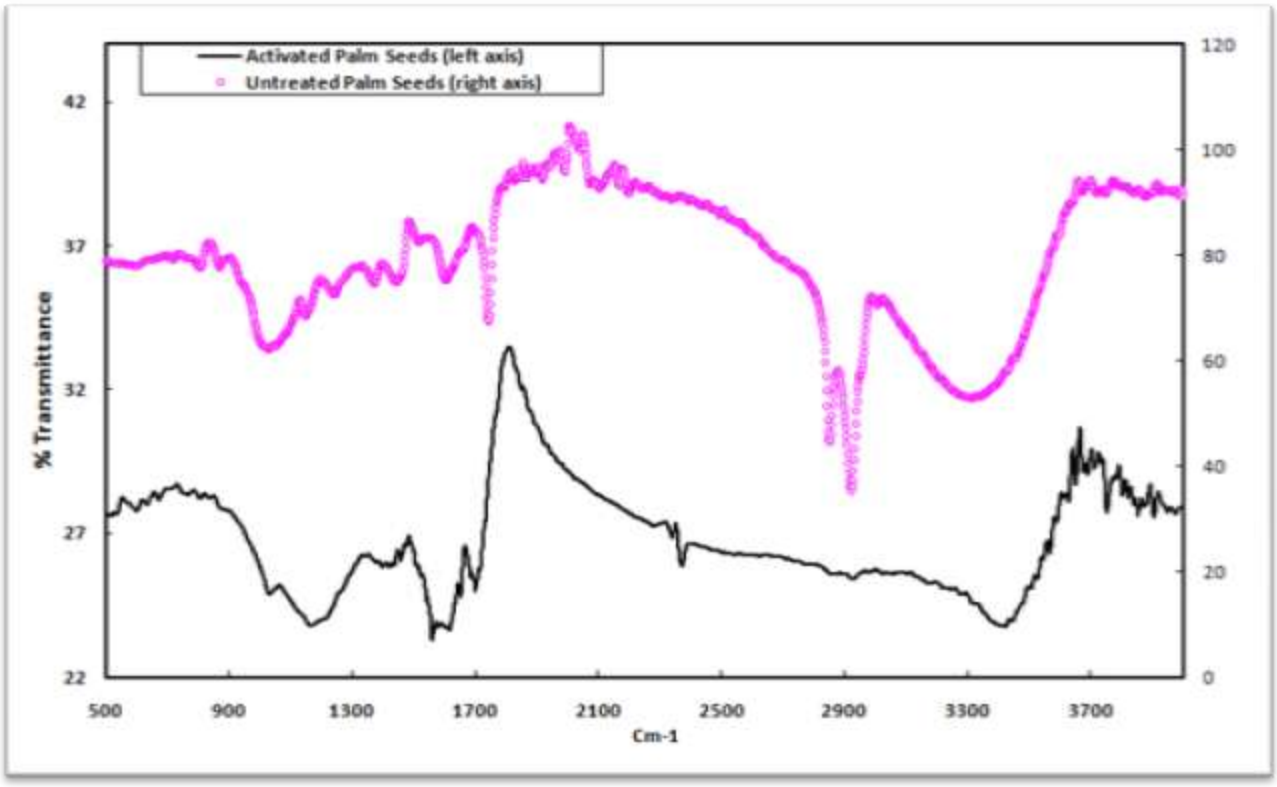

Figure 4.11- FTIR spectrum for activated carbon (J5)

FTIR analyses the activated carbon (K5) is shown in Figure 4.12. Two peaks at 3852.0 and 3750.0 cm^{-1}, appeared after activation which are assigned to the O-H stretching mode of hydroxyl groups and adsorbed water. Also a new peak at 3418.6 cm^{-1} appeared after activation which is attributed to the presence of (C≡C) group. On the other hand, the peaks at 1700.2 cm^{-1} are related to (C=O) group. The intensity of the peak at 806.8 is referred to alkenes (=CH) and ($=CH_2$).

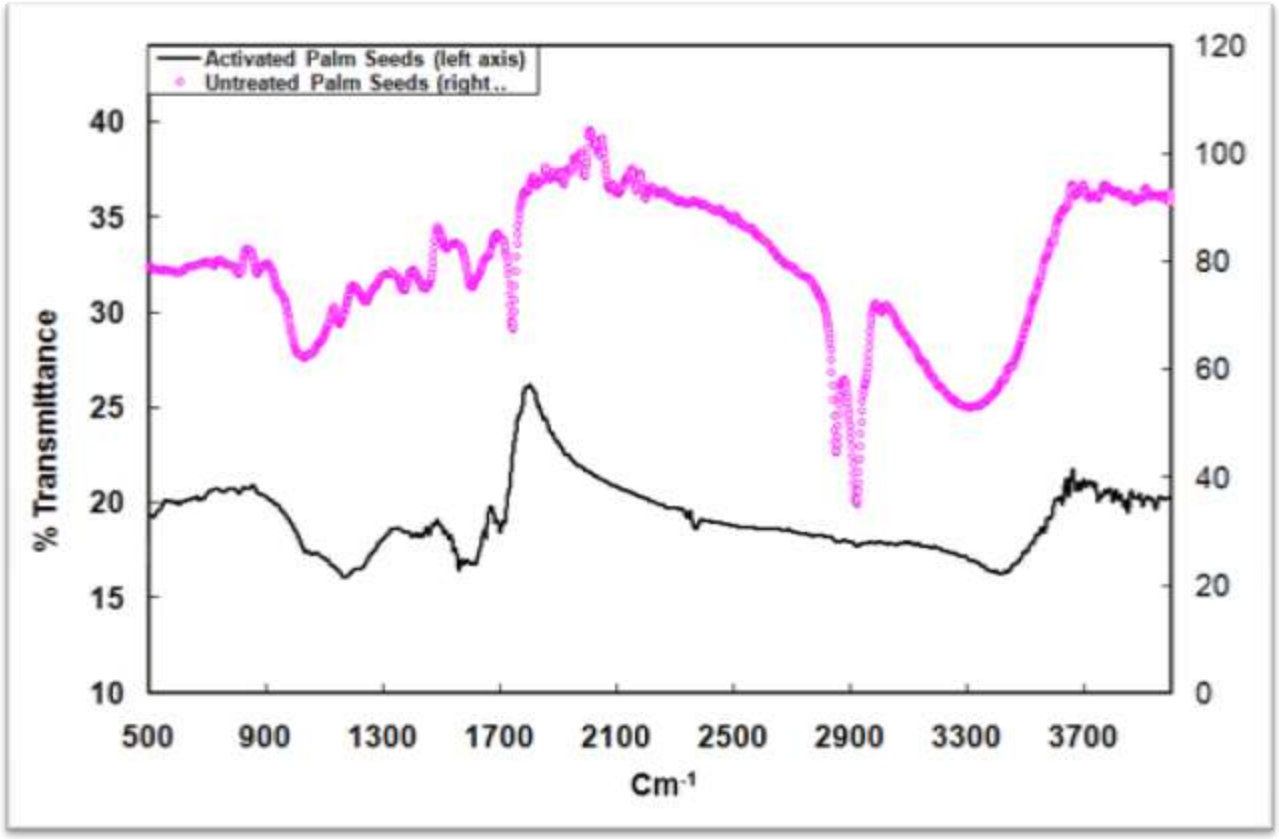

Figure 4.12- FTIR spectrum for activated carbon (K5)

4.2 Adsorption of 4-Chlorophenol from Aqueous Solution on Activated Carbon Surface

Removal of 4-Chlorophenol (4-CP) by adsorption on activated carbon surface was tested and investigated in this project. Several factors and variables affecting this removal were studied and investigated in terms of isotherm and batch kinetic studies. These factors include initial sorbate concentration, mass of adsorbent, pH of sorbet's solution and sorbate solution's temperature.

Adsorption isotherm maps the distribution of adsorbate solute between the liquid and solid phases at various equilibrium concentrations. Also, it is based on data that are specific for each system and must be determined for each equilibrium system. Moreover, different shapes of adsorption isotherms are due to different porous structures of adsorbents and adsorbate-adsorbent interactions. Adsorption isotherm is a graphical representation showing relationship between the amount adsorbed by a unit weight of adsorbent and adsorbate remaining in the test medium at equilibrium [38].

4.2.1 Adsorption Isotherm of 4-Chlorophenol

Adsorption isotherm of 4-CP versus BET IS shown in figure 4.13. The amount of adsorbate that adsorbed on the activated carbon surface, q (mg/g), was calculated according to the following equation:

$$q_e = \frac{a_o a_1 C_e}{(a_2 - C_e)\left[1 + \frac{(a_o - 1)C_e}{a_2}\right]}$$

C_e: Equilibrium adsorbate concentration (mg/l)

q_e; Adsorbed solute volume per adsorbent unit mass at equilibrium (mg/g)

BET isotherm is based on several assumptions which are the following.

1- Multilayer adsorption

2-Each layer of adsorbate is treated as a Langmuir monolayer and each layer must be completed before the next layer starts to form.

3- The heat of adsorption for the first layer is characteristic of the adsorbate adsorbent system.

4- The heat of adsorption for subsequent layers is equal to the heat of condensation

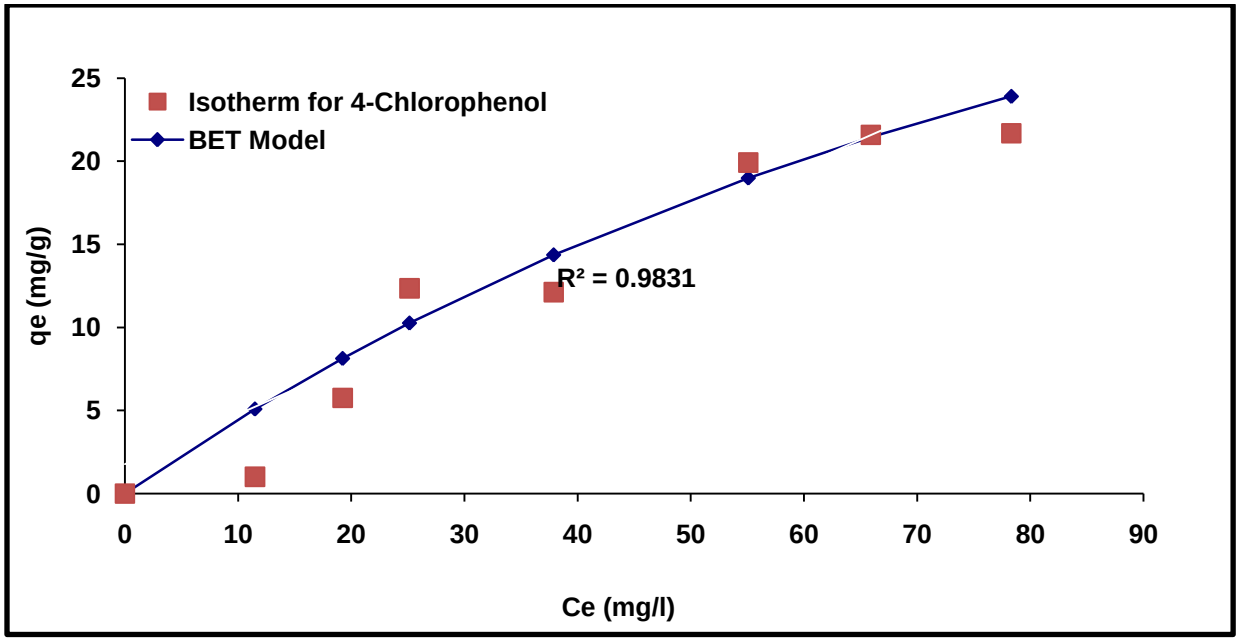

Figure 4.13-Experimetnal and Theoretical Adsorption Isotherm of 4-CP on Activated Carbon

4.2.2 Adsorption Kinetics of 4-Chlorophenol Adsorption

The kinetic studies for 4-CP involve several factors that influence 4-CP adsorption on activated carbon surface. These factors include initial adsorbate solution concentration, adsorbent mass, adsorbate solution's pH and adsorbate solution's temperature.

4.2.2.1 Effect of Initial Adsorbate Concentration

The effect of initial concentration (C_o) of 4-CP solution on its adsorption onto activated carbon surface was investigated at different concentration values 100, 200 and 300 ppm. Figure 4.14 represents the experimental kinetic curves for different initial concentrations for 4-Chlorophenol (100, 200 and 300 ppm) and their concentrations after adding the adsorbent into their solutions.

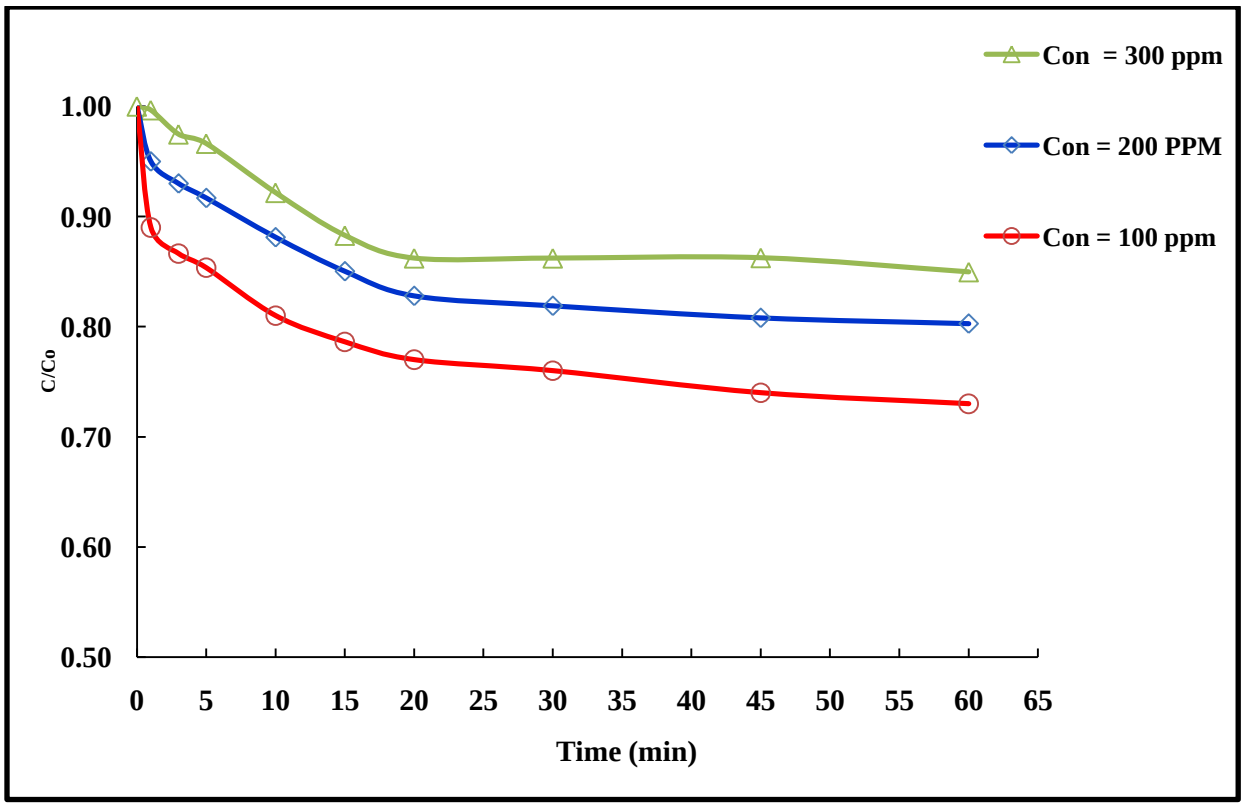

Figure 4-14. Effect of Initial Concentration on 4-CP Adsorption on Activated Carbon

Obviously, increasing initial adsorbate concentration leads to a decrease in the adsorption capacity of the adsorbent. Also, figure 4.14 shows that as the initial concentration increases, the adsorption of adsorbate increases but as soon as all of the sites on the activated carbon surface are occupied, a further increase in adsorbate concentration will not increase the amount adsorbed onto the adsorbent surface.

4.2.2.2 Effect of Adsorbent Mass

The effect of adsorbent mass on the adsorption process of 4-CP on activated carbon surface was investigated using different adsorbent's masses (1, 2 and 3g). Figure 4.15 shows kinetic curves for the effect of the adsorbent mass (m) on the kinetics of 4-CP adsorption on activated carbon. It is clear that as the adsorbent mass increases the removal of 4-CP removed increases too. For one gram mass of adsorbent 15 milligrams of 4-CP were removed and 34 milligrams were removed by 2 grams mass of adsorbent (17 mg/g). Finally, 39.4 milligrams of 4-CP were removed by three grams adsorbent mass (13.13 mg/g).

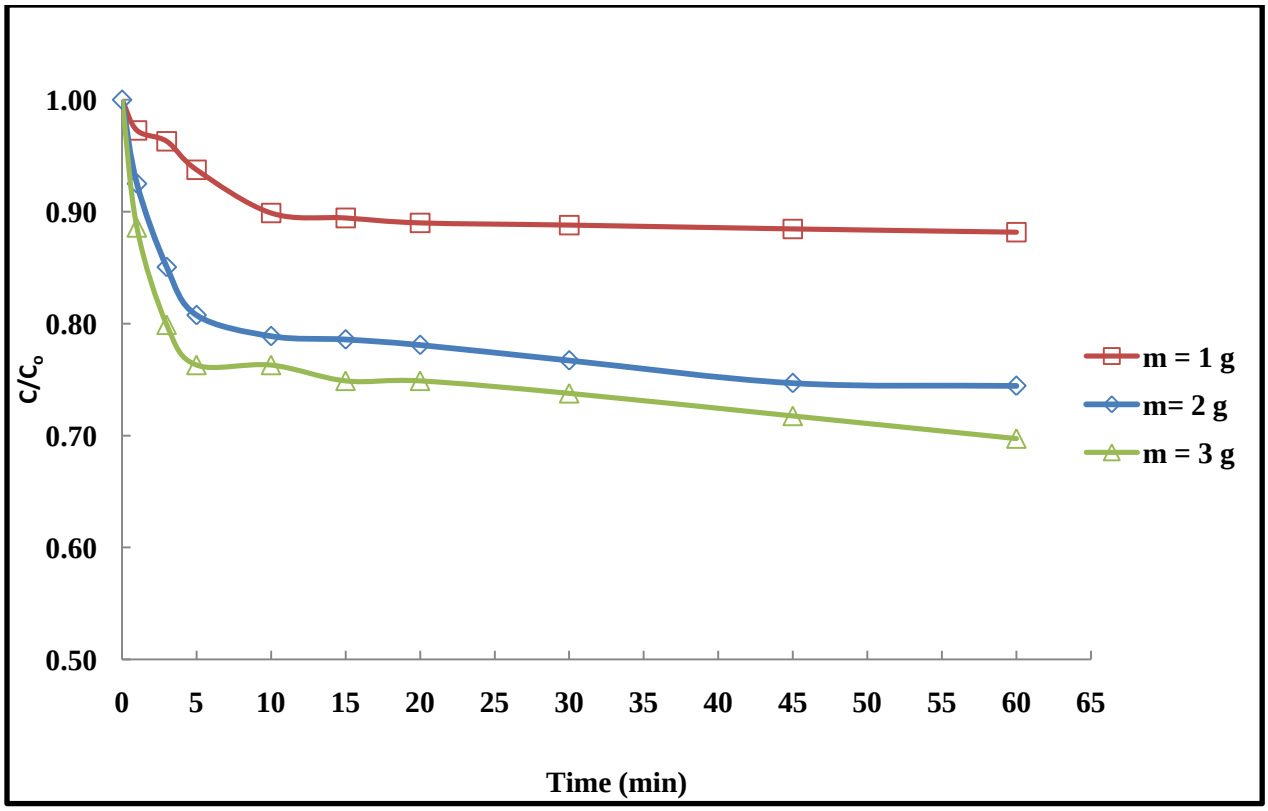

Figure 4.15: Effect of adsorbent mass on 4-CP adsorption on activated carbon

Increasing adsorbent mass will increase the surface area available for sorption. Consequently, rate of 4-CP uptake increases. Koumanova obtained the same results [43].

4.2.2.3 Effect of Adsorbate's pH

The influence of pH on the yield of 4-CP removal was carried out for a solution that has pH in a range of 4-11. The solution's pH adjustment was realized by using an acid (nitric acid) or a base (sodium hydroxide). As figure 4.16 shows, the maximum uptake of 4-CP took place at pH=4.0. For solution that has pH of 4.0, 17.0 mg/g was removed while only 13.5 mg/g of 4-CP was removed for solution of pH 9.0. Long and Pinto concluded that the phenol uptake increases upon the removal of the carboxylic functional groups from the carbon surface as a result of decreased competitive adsorption of water molecules on the basal planes of the carbon [44]

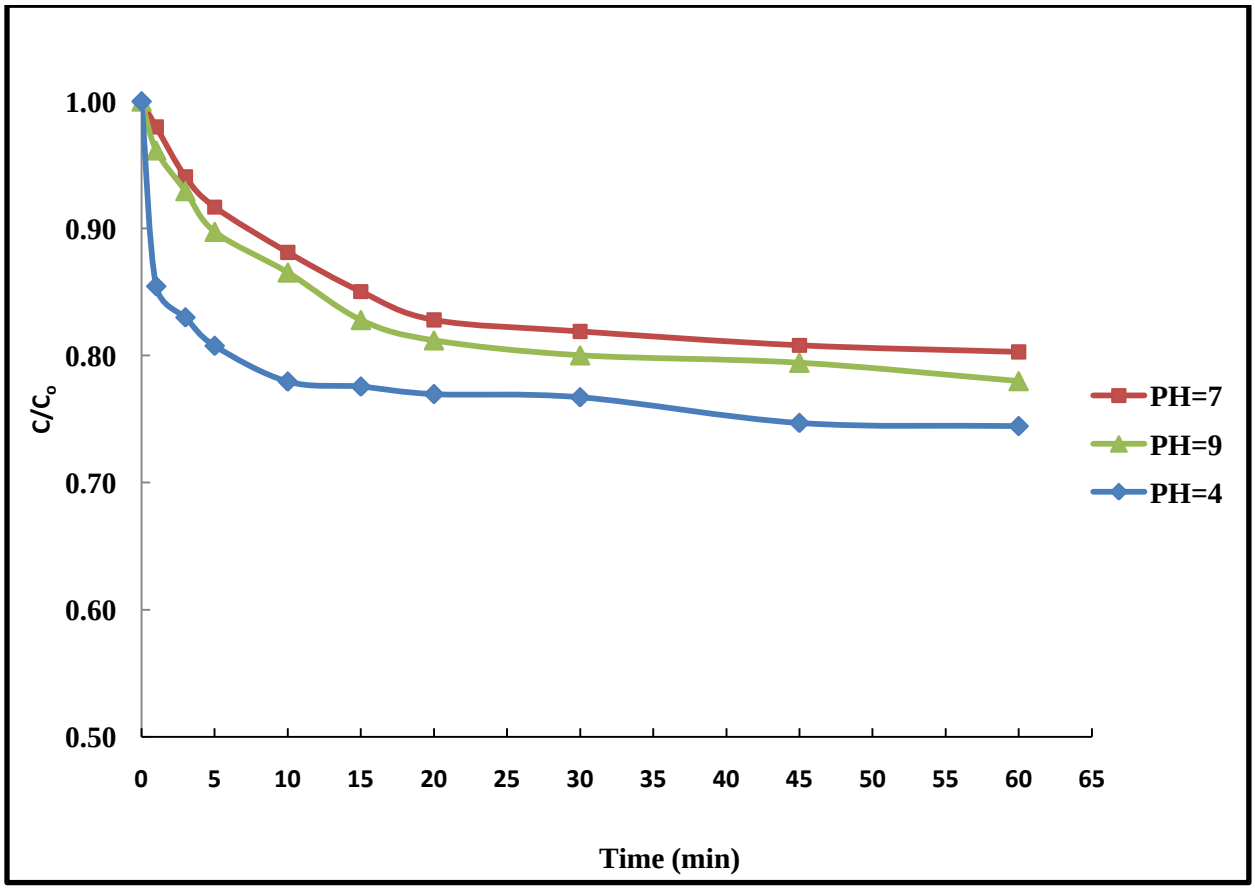

Fig 4.16- Effect of Adsorbate pH on 4-CP Adsorption

At low pH values the presence of H^+ ions suppresses the ionization of adsorbate and hence its uptake on the adsorbent surface. At higher pH range, adsorbate forms salts that readily ionize leaving the negative charge on the adsorbate (phenolic) group. At the same time the presence of OH^- ions on the adsorbent prevents the binding of phenoate that leads to low phenol adsorption [13].

Another reason for decreasing the adsorption of 4-chlorophenol with increasing the solution pH is due to the increased solubility of 4-chlorophenol molecules to remain in solution rather than to get adsorbed onto the activated carbon surface. Hannafi et al. concluded that the maximum adsorption is obtained towards a pH =5.5 in their study [29]. Moreover, the removal of phenol by activated carbon prepared from leaf litter increase in pH range 2-6 [13]. The uptake of 4-CP decreases at lower pH values as well as higher pH [7-8].

4.2.2.4 Effect of Adsorbate Temperature

Temperature is a main factor in adsorption processes since it affects the solubility of adsorbents and the adsorption equilibrium constant. In this work five different temperatures were tested 1, 10, 22, 35 and 50 ^oC. Other remaining factors were fixed during these tests (pH=7.0, adsorbent mass= 2.0 g and adsorbate concentration 200 ppm, solution volume 1.7 liter).

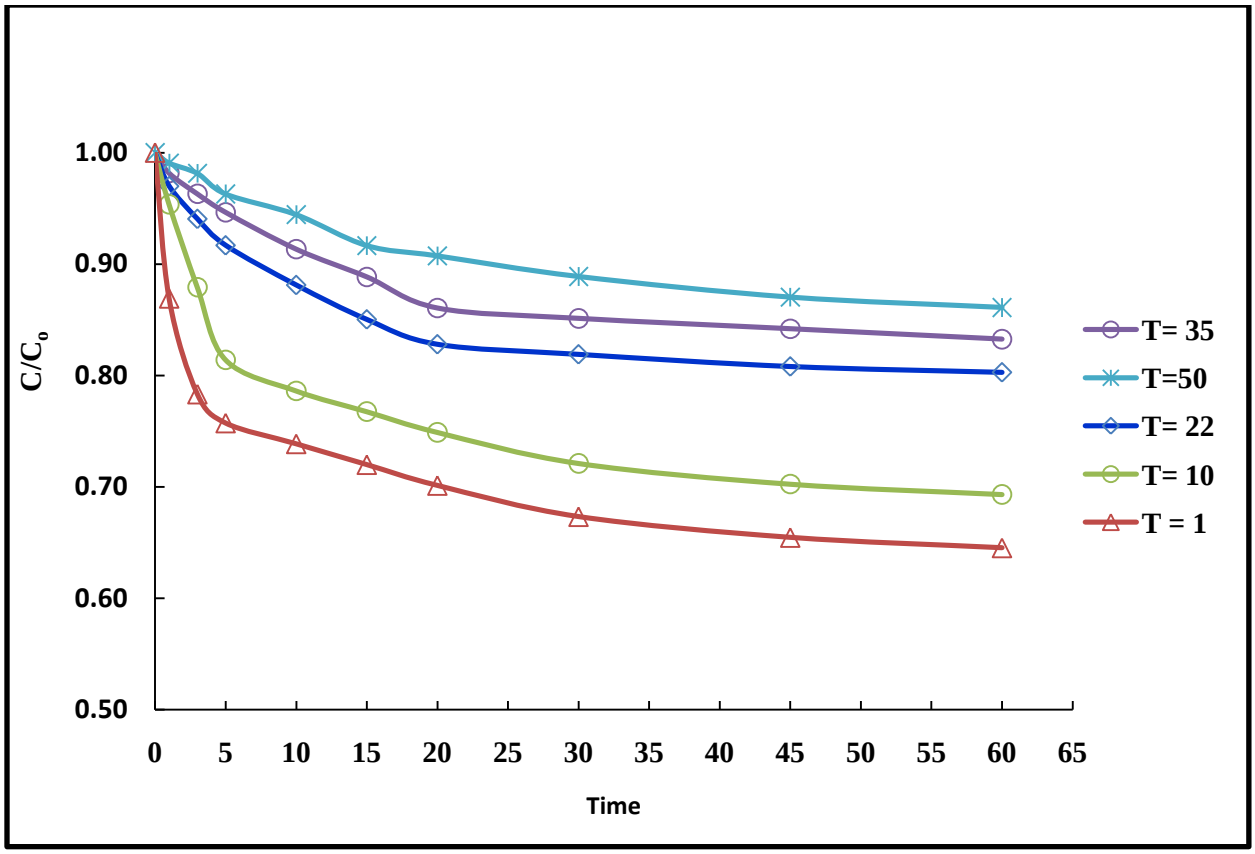

Figure 4.17-Effect of adsorbate temperature on 4-CP adsorption

Figure 4.17 shows the effect of temperature on adsorption process. It can be seen that a decrease in the adsorption capacity when temperature was risen which is in contradiction with the expected trend of any physical adsorption. It was expected that the adsorption capacity would increase by increasing the solute temperature.

Determining some thermodynamic parameters such as standard enthalpy (ΔH^o), standard entropy (ΔS^o) and standard free energy (ΔG^o) can determine the nature of the process from thermodynamics point of view. The previous parameters can be computed using the following equation.

$$\ln k_d = \frac{\Delta S^o}{R} - \frac{\Delta H^o}{RT}$$

K_d: Distribution Coefficient

R: Gas Constant (8314 J/mol K)

T: Temperature (K)

ΔS^o : Standard Entropy (J/K)

ΔH^o: Standard Enthalpy (J)

$$\mathbf{K_d} = \frac{q_e}{C_e}$$

Where q_e (mg/g) is the amount adsorbed on solid at equilibrium and C_e (mg/l) is the equilibrium concentration. The values of ΔH^o and ΔS^o are calculated from the slope and intercept of van't Hoff plots of ln K_d versus 1/T as shown in figure 4.18 [39].

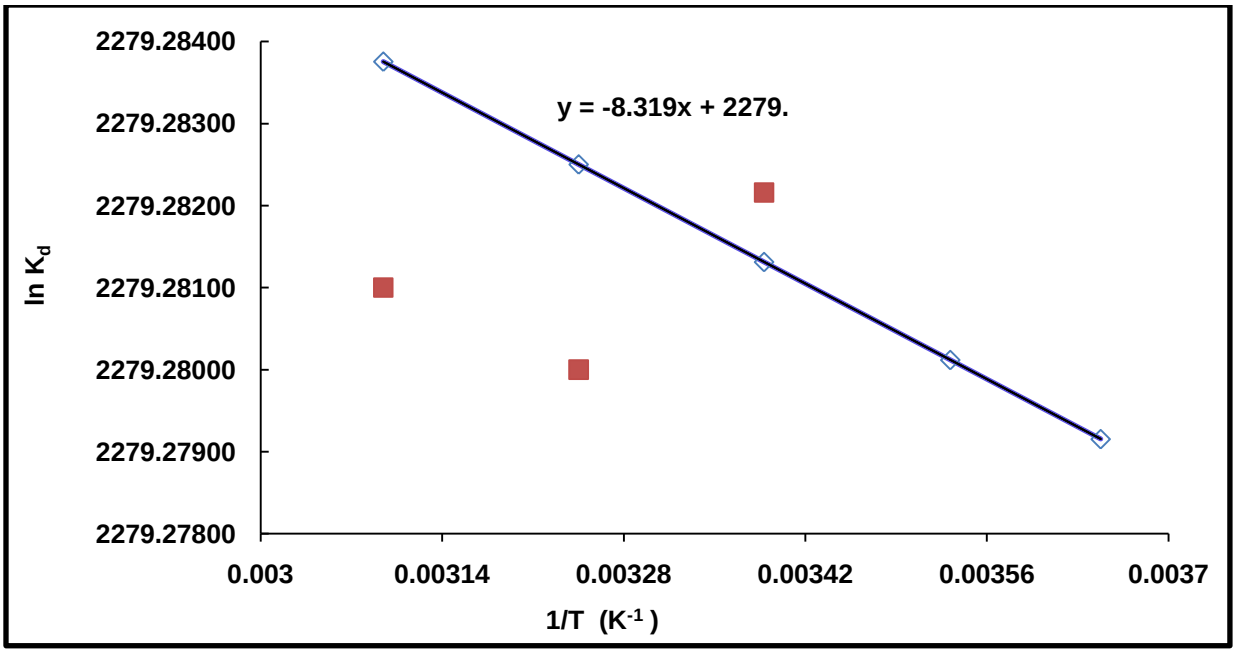

Figure 4.18-ln K_d versus 1/T for 4-CP adsorption on activated carbon surface

The exothermic nature of the process is supported by the negative value of ΔH^o (-16.53 Kcal/mol)., while the value of standard enthalpy is (4828.9 Kcal/K).

CHAPTER 5

5. CONCLUSION and RECOMMENDATIONS

5.1 Conclusions

Synthesis of activated carbon was carried out by two different activation methods namely chemical and physical activation. The resulted activated carbon was characterized for several parameters such as BET, SEM, ZPC and FTIR. After characterization the highest BET surface area activated carbon was utilized for the removal of 4-chlorophenol from aqueous solution under different experimental conditions. The following were concluded based on the experimental results of this research:

5.1.1 Chemical Activation:

1. As the volume ratio of nitric acid to phosphoric acid increases the yield decreases.
2. The yield decreases with increasing the nitric acid to palm seeds ratio.
3. As the volume ratio of phosphoric to nitric acid increases the bulk density increases too.

5.1.2 Physical Activation

1. As physical activation temperature increases the yield decreases.

5.1.3 Characterization of Activated Carbon:

1. The highest BET surface area activated carbon sample was the sample that chemically activated using phosphoric acid and 550 ^{o}C temperature.

5.1.4 Adsorption of 4-Chlorophenol on Activated Carbon Surface:

1. As initial concentration of 4-CP increases, its removal increases until all sites on the activated carbon surface are occupied, a further increase in adsorbate concentration would not increase the amount adsorbed on the surface.
2. The maximum uptake of 4-Chlorophenol takes place at pH=4.
3. As adsorbent mass increases, the concentration of 4-CP decreases until it reaches to equilibrium point when it stays constant.
4. The adsorption processes of 4-CP on activated carbon surface decreases with increasing the temperature suggesting that these process are exothermic process.

5.2 Recommendations

The following recommendations could be useful for future work and research:

1. More oxidizing agents can be utilized and tested with different volume ratios in chemical activation stage.

2. Physical activation can be carried out at higher temperatures to evaluate its impact on BET surface area. Also, use different fluid such as steam or nitrogen with different flow rates.

3. Utilize the subject activated carbon to remove non-organic solutes such as metals.

References

1 Shawabkeh, R. and Abu-Nameh, E. Absorption of phenol and methylene blue by activated carbon from pecan shells. Colloid Journal, 2007, 69(3), 355-359.

2 Mishra, S. and Bhattacharya, J. Batch Studies on Phenol Removal using Leaf Activated carbon. Malaysian Journal of Chemistry, 2007, 9(1), 051-059.

3 Tan, I.A.W., Ahmad, A.L. and Hameed, B.H. Enhancement of basic dye adsorption uptake from aqueous solutions using chemically modified oil palm shell activated carbon. Colloids and Surfaces A: Physicochemical and Engineering Aspects, 2008, 318(1-3), 88-96.

4 Tan, I.A.W., Hameed, B.H. and Ahmad, A.L. Equilibrium and kinetic studies on basic dye adsorption by oil palm fibre activated carbon. Chemical Engineering Journal, 2007, 127(1-3), 111-119.

5 Shawabkeh, R., Al-Harahsheh, A., Hami, M. and Khlaifat, A. Conversion of oil shale ash into zeolite for cadmium and lead removal from wastewater. Fuel, 2004, 83(7-8), 981-985.

6 Shawabkeh, R.A. and Tutunji, M.F. Experimental study and modeling of basic dye sorption by diatomaceous clay. Applied Clay Science, 2003, 24(1-2), 111-120.

7 Shawabkeh, R., Al-Khashman, O., Al-Omari, H. and Shawabkeh, A. Cobalt and zinc removal from aqueous solution by chemically treated bentonite. The Environmentalist, 2007, 27(3), 357-363.

8 Shawabkeh, R.A. Synthesis and characterization of activated carbo-aluminosilicate material from oil shale. Microporous and Mesoporous Materials, 2004, 75(1-2), 107-114.

9 Wang, Y., Huang, Z., Liu, Z. and Liu, Q. A novel activated carbon honeycomb catalyst for simultaneous SO2 and NO removal at low temperatures. Carbon, 2004, 42(2), 445-448.

10 Ranganathan, K. Chromium removal by activated carbons prepared from Casurina equisetifolia leaves. Bioresource Technology, 2000, 73(2), 99-103.

11 Park, S.-J. and Jung, W.-Y. Effect of KOH Activation on the Formation of Oxygen Structure in Activated Carbons Synthesized from Polymeric Precursor. Journal of Colloid and Interface Science, 2002, 250(1), 93-98.

12 Ng, C., Losso, J.N., Marshall, W.E. and Rao, R.M. Freundlich adsorption isotherms of agricultural by-product-based powdered activated carbons in a geosmin-water system. Bioresource Technology, 2002, 85(2), 131-135.

13 Shim, J.-W., Park, S.-J. and Ryu, S.-K. Effect of modification with HNO3 and NaOH on metal adsorption by pitch-based activated carbon fibers. Carbon, 2001, 39(11), 1635-1642.

14 Chen, Y., Yang, H. and Gu, G. Effect of acid and surfactant treatment on activated sludge dewatering and settling. Water Research, 2001, 35(11), 2615-2620.

15 Dastgheib, S.A. and Rockstraw, D.A. A model for the adsorption of single metal ion solutes in aqueous solution onto activated carbon produced from pecan shells. Carbon, 2002, 40(11), 1843-1851.

16 Bodoev, N.V., Gruber, R., Kucherenko, V.A., Guet, J.-M., Khabarova, T., Cohaut, N., Heintz, O. and Rokosova, N.N. A novel process for preparation of active carbon from sapropelitic coals. Fuel, 1998, 77(6), 473-478.

17 Ayranci, E. and Conway, B.E. Removal of phenol, phenoxide and chlorophenols from waste-waters by adsorption and electrosorption at high-area carbon felt electrodes. Journal of Electroanalytical Chemistry, 2001, 513(2), 100-110.

18 Schwegler, M.A., Vinke, P., van der Eijk, M. and van Bekkum, H. Activated carbon as a support for heteropolyanion catalysts. Applied Catalysis A: General, 1992, 80(1), 41-57.

19 Jiang, Z., Liu, Y., Sun, X., Tian, F., Sun, F., Liang, C., You, W., Han, C. and Li, C. Activated Carbons Chemically Modified by Concentrated H2SO4 for the Adsorption of the Pollutants from Wastewater and the Dibenzothiophene from Fuel Oils. Langmuir, 2003, 19(3), 731-736.

20 Yamashita, J., Shioya, M., Kikutani, T. and Hashimoto, T. Activated carbon fibers and films derived from poly(vinylidene fluoride). Carbon, 2001, 39(2), 207-214.

21 Hamadi, N.K., Chen, X.D., Farid, M.M. and Lu, M.G.Q. Adsorption kinetics for the removal of chromium(VI) from aqueous solution by adsorbents derived from used tyres and sawdust. Chemical Engineering Journal, 2001, 84(2), 95-105.

22 Demirbas, E., Kobyab, M., Senturkb, E. and Ozkana, T. Adsorption kinetics for the removal of chromium (VI) from aqueous solutions on the activated carbons prepared from agricultural wastes. Water SA, 2004, 30, 533-539.

23 Boudou, J.P., Mariadassou, G.D., Begin, D., Alain, E., Marêché, J.F., Furdin, G., Siemieniewska, T. and Albiniak, A. Activated carbons from mixtures of coal pitch and FeCl3---graphite intercalated compounds. Journal of Physics and Chemistry of Solids, 57(6-8), 753-759.

24 Guo, J. and Chong Lua, A. Characterization of chars pyrolyzed from oil palm stones for the preparation of activated carbons. Journal of Analytical and Applied Pyrolysis, 1998, 46(2), 113-125.

25 Nguyen, T.X. and Bhatia, S.K. Characterization of activated carbon fibers using argon adsorption. Carbon, 2005, 43(4), 775-785.

26 Rodríguez-Reinoso, F. and Molina-Sabio, M. Activated carbons from lignocellulosic materials by chemical and/or physical activation: an overview. Carbon, 1992, 30(7), 1111-1118.

27 Bansode, R.R., Losso, J.N., Marshall, W.E., Rao, R.M. and Portier, R.J. Adsorption of volatile organic compounds by pecan shell- and almond shell-based granular activated carbons. Bioresource Technology, 2003, 90(2), 175-184.

28 Montilla, F., Morallón, E., Vázquez, J.L., Alcañiz-Monge, J., Cazorla-Amorós, D. and Linares-Solano, A. Carbon-ceramic composites from coal tar pitch and clays: application as electrocatalyst support. Carbon, 2002, 40(12), 2193-2200.

29 Malik, D.J., Strelko, V.J., Streat, M. and Puziy, A.M. Characterisation of novel modified active carbons and marine algal biomass for the selective adsorption of lead. Water Research, 2002, 36(6), 1527-1538.

30 Hu, Z. and Vansant, E.F. Chemical activation of elutrilithe producing carbon-aluminosilicate composite adsorbent. Carbon, 1995, 33(9), 1293-1300.

31 Aksoylu, A.E., Freitas, M.M.A. and Figueiredo, J.L. Bimetallic Pt-Sn catalysts supported on activated carbon. II. CO oxidation. Catalysis Today, 2000, 62(4), 337-346.

32 Yang, T. and Lua, A.C. Characteristics of activated carbons prepared from pistachio-nut shells by potassium hydroxide activation. Microporous and Mesoporous Materials, 2003, 63(1-3), 113-124.

33 Efremenko, I. and Sheintuch, M. Carbon-supported palladium catalysts. Molecular orbital study. Journal of Catalysis, 2003, 214(1), 53-67.

34 Yang, T. and Lua, A.C. Characteristics of activated carbons prepared from pistachio-nut shells by physical activation. Journal of Colloid and Interface Science, 2003, 267(2), 408-417.

35 Gournis, D., Karakassides, M.A., Bakas, T., Boukos, N. and Petridis, D. Catalytic synthesis of carbon nanotubes on clay minerals. Carbon, 2002, 40(14), 2641-2646.

36 Hu, Z. and Vansant, E.F. Carbon molecular sieves produced from walnut shell. Carbon, 1995, 33(5), 561-567.

37 Strelko, V., Malik, D.J. and Streat, M. Characterisation of the surface of oxidised carbon adsorbents. Carbon, 2002, 40(1), 95-104.

38 Aguilar, C., García, R., Soto-Garrido, G. and Arriagada, R. Catalytic wet air oxidation of aqueous ammonia with activated carbon. Applied Catalysis B: Environmental, 2003, 46(2), 229-237.

39 Laszlo, K., Josepovits, K. and Tombacs, E. Analysis of active sites on synthetic carbon surfaces by various methods. Analytical Science, 2001, 17, 1741-1744.

NOMENCLATURE

M_{before}: Mass of activated carbon before washing (g)

M_{after}: Mass of activated carbon after washing (g)

M: Initial mass of palm seeds (g)

M: Mass of adsorbate (g)

f (γ): Pore volume distrubution

C_o: Initial adsorbate concentration (mg/l)

C_e: Equilibrium adsorbate concentration (mg/l)

q: Amount of adsorbate adsorbed per unit mass of adsorbent (mg/g)

Q_e: Amount of adsorbate adsorbed per unit mass of adsorbent (mg/g)

R_L: Langmuir constant

C_0: Initial Concentration (ml/ liter)

V: Volume of the solution (liter)

R: Universal Gas constant

T: Solution temperature (K)

K_d: Distribution Coefficient

ΔS^o: Standard Entropy (J/K)

ΔH^o: Standard Enthalpy (J)

VITA

Name	Saeed Mohammad Al-Ghamdi
Religion	Islam
Nationality	Saudi
Place and Date of Birth	Baha, Saudi Arabia, May 1979
Address	Saudi Aramco Company Saudi Aramco Box 1995, Ras Tanura 8260, Saudi Arabia Ras Tanura, Eastern Province, Saudi Arabia
E-mail Address	ghamsm17@aramco.com.sa
Contact information	Office: +966 3 678-9045 Fax: +966 3 678-9262 Mobile: +966 503834714
Education	Bachelor of Science in Chemical Engineering from King Fahd University of Petroleum & Minerals in February 2003
	Master of Science in Chemical Engineering from King Fahd University of Petroleum & Minerals in April 2011.
Publication	Shawabkeh, R. et al., Synthesis and characterization of Microporoes, High Surface Area Activated Carbon from Palm Seeds. Energy Sources, 2012.